CHAPTER 3

EXPERIMENTAL INVESTIGATION AND RESULTS

The purpose of this experiment aims at understanding the hydrodynamics of drops in spray columns, and attempt at increasing understanding or even predicting hydrodynamics of drop in other spray columns. The results of this experiments were compared with other investigator's equations. Most of this experimental study deals with photographs of drops to estimate drop characteristics and drop dynamics. The details of the experimental investigation and results are presented as follow.

3.1 Experimental Investigation

3.1.1 Apparatus

The general arrangement of the apparatus used is shown in figure 1. The main experimental apparatus consisted of the follow items.

3.1.1.1 A 11.2 cm. diameter by 133 cm. column and accessories.

3.1.1.2 Measuring and auxiliary equipment.

3.1.1.1 Column: The glass column used in this experiment was 133 cm. long with an inside diameter of 11.2 cm. The column was built in 5 glass sections of about 26.6 cm. long with several plexiglass flanges used to join the column sections together.

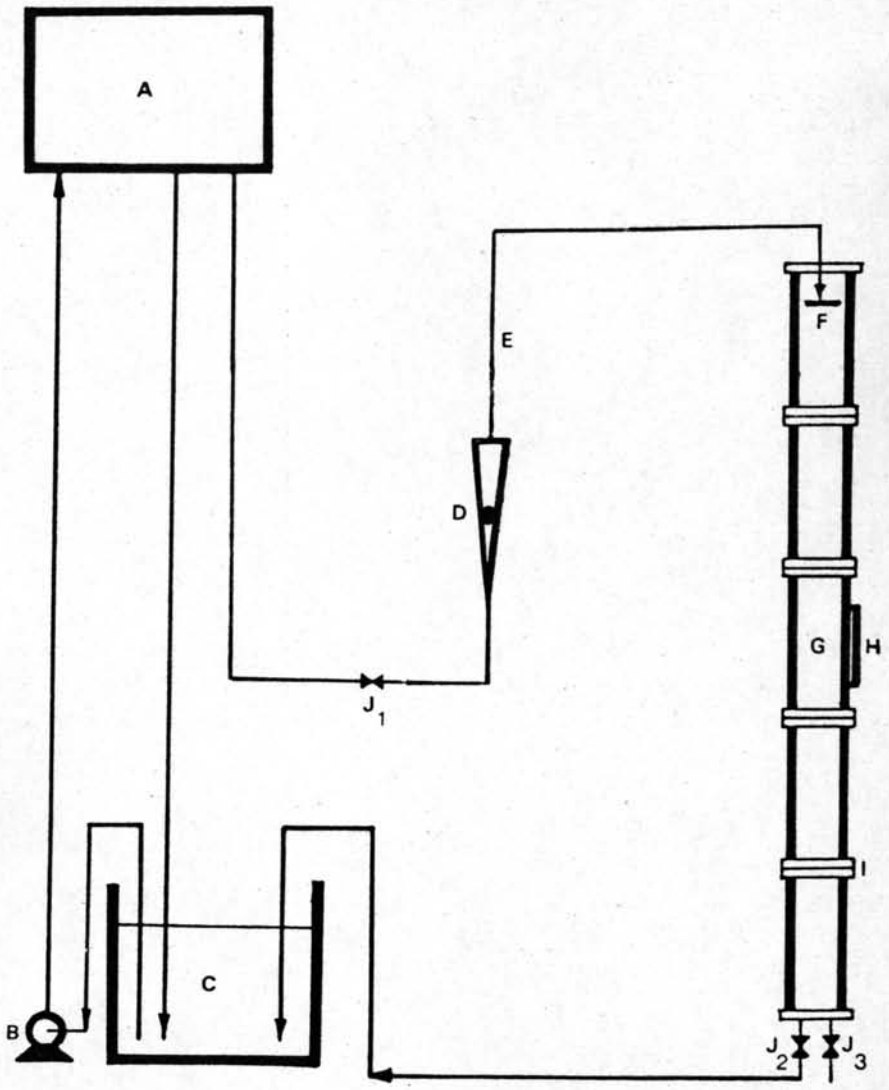

Figure 1 Schematic representation of the Spray Column.

A Head Tank, B Micro-Pump, C Storage Tank,

D Rotameter, E Carbon Tetrachloride Feed Pipe,

F Distributor, G Photography Section,

H Perspex Box, I Plexiglass Flanges, J Valve,

3.1.1.2 Measuring and auxiliary equipment.

1. Rotameter: A glass ball rotameter was used to measure flow rates of dispersed phase (carbon tetrachloride). The flow rate of this rotameter could be varied between 0 and 60 liter/hr.

2. Pump: A Micro-Pump 230 V, 0.5 A was used to pump dispersed phase to the head tank in order to maintain a constant head.

3. Distributor: An aluminium perforated plate was used to introduce dispersed phase drops into the column. The dispersion of dispersed phase was done using four sets of distributor nozzles, varying in numbers and sizes, the complete characteristics of which are presented in table 2.

Table 2 Nozzle characteristics

Distributor No.	Nozzle diameter mm.	No. of nozzles	Free area of passage $mm.^2$
A	1.5	17	30.04
B	2.0	9	28.27
C	2.5	6	29.45
D	3.0	4	28.27

4. Camera: A Canon FT_b 50 mm., 1:1.4 was used to photograph the drops as they formed in the column. All photographs were taken through a No. plus 1, 2 and 4 Vivitar lens connected together to make close-up possible.

5. Bright light source: A Fuji lamp photographic reflector 230 V, 500 W. for a bright light source was used to take pictures of the drops.

6. Film: The film used was black and white Fuji film Neopan SS ASA 100.

3.1.2 Procedure

The column was first filled with water from the top of the column. Carbon tetrachloride in storage tank C was pumped to head tank A used to maintain constant flow. Carbon tetrachloride flowed by gravity from storage tank A to rotameter D and distributor F. The rotameter was used only to vary flow rates, and the available head changed little during the course of a run and no difficulties were encountered in maintaining constant velocity. Drops of carbon tetrachloride formed at distributor F would fall through the column and collected in a layer at the bottom, then drained by valve J_2 into storage tank C.

A perspex box H filled with water was fitted on to the column. A camera was used to photograph the drops in section G. Drop sizes and velocities of drops were measure using photography.

The arrangement used for photographing the droplets for drop size measurements and velocity of drop measurements are shown schematically in Figures 2 and 3. All photographs were obtained when the column was operating under steady state conditions.

During the measurement of drop sizes the flow rate of carbon tetrachloride was varied between the values 8.68, 6.67, 5.03

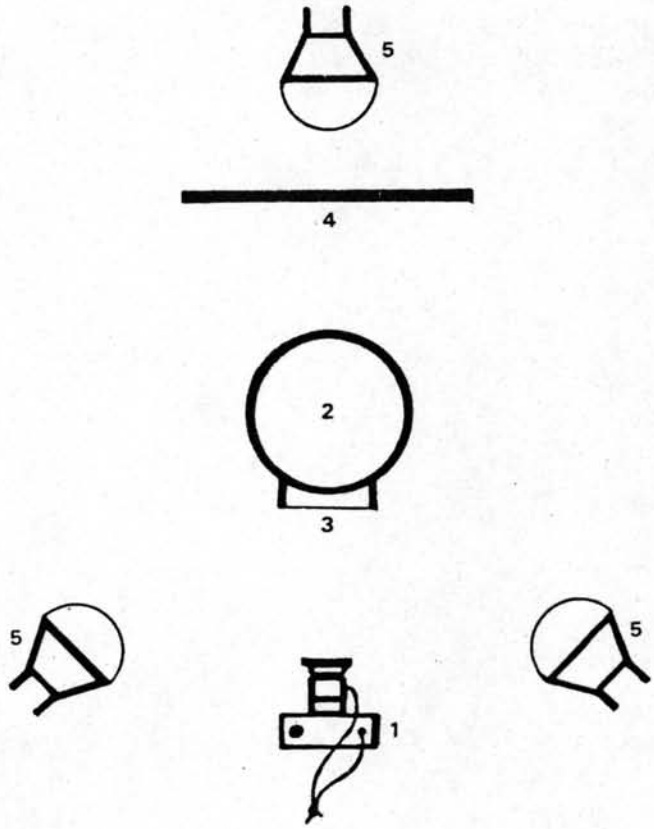

Figure 2 Experimental photographic set up to measure drop sizes

1. Canon FT_b camera with close-up lens
2. Spray Column
3. Perspex box
4. Frosted diffuser glass plate
5. 500 W light sources.

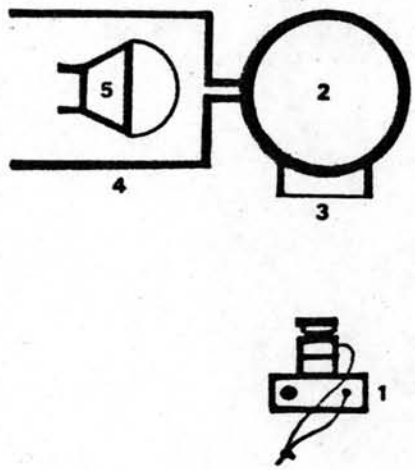

Figure 3 Experimental photographic set up to measure velocities of drops

1. Canon FT_b camera with close-up lens
2. Spray column
3. Perspex box
4. Light shield with 0.5 cm slit
5. 500 W light source

and 3.37 cc./s, using distributors A, B, C and D respectively. Exposures of 0.001 second, and a lens opening f11 were used. This produced sharp outlines at all flow rates. Usually 15 to 20 photographs were taken at low flow rates and 10 to 15 at high flow rates. Samples of photographs of drops of various sizes are shown on figure 4 to 7.

To enable measurements of velocities of drops, the flow rate of carbon tetrachloride was varied from 8.68, 6.67 and 5.03 cc./s respectively, and distributors A, B, C and D were used. A 500 W light source was allowed through a 0.5 cm. slit made of aluminium sheets, such an arrangement allowed a thin ray of light to pass through the center of the column. A camera lens opening of f 1.4, and a 1/30 second exposure time was used during this particular set of experiments. Usually approximately 340 photographs were taken at low flow rates and approximate 230 at high flow rates. Sample photographs of drop are shown on figure 8 to 11.

The negatives of these photographs were studied with the help of a slide projector which enlarged the images 20 to 25 times, and measured using as reference a tube of known dimensions placed within the column as dimension reference.

The method of obtaining drop sizes used is based on calculation of horizontal and vertical diameters of drops from the true length of major and minor axes d_1 and d_2 respectively. The equivalent volume diameter of the corresponding spherical droplets was calculated from the equation.

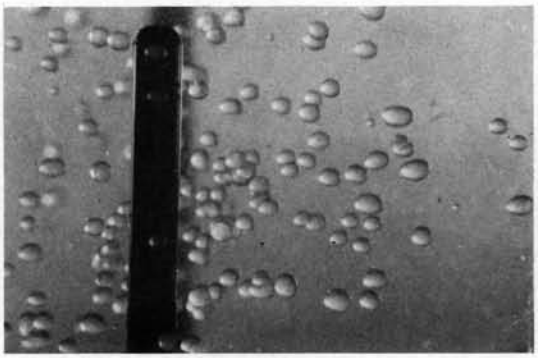

a

Q_d = 8.68 cc./s.

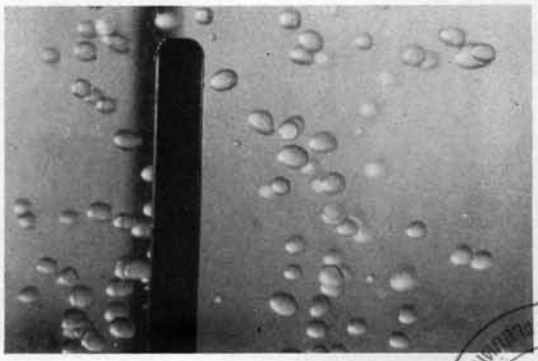

b

Q_d = 6.67 cc./s.

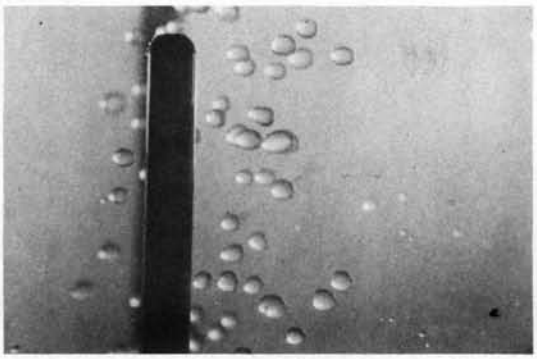

c

Q_d = 5.03 cc./s.

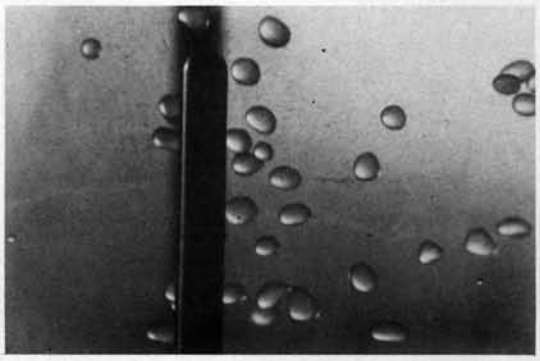

d

Q_d = 3.37 cc./s.

Figure 4 Photographs of drops sizes with varying flow rates of dispersed phase (distributor A)

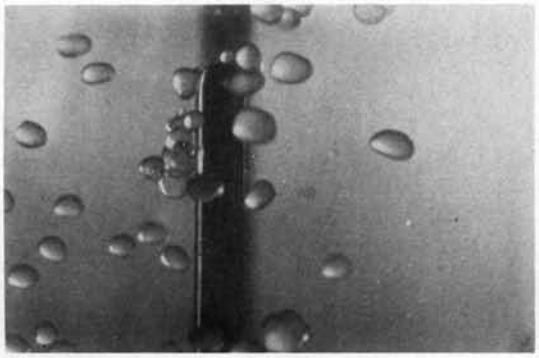

a

Q_d = 8.68 cc./s.

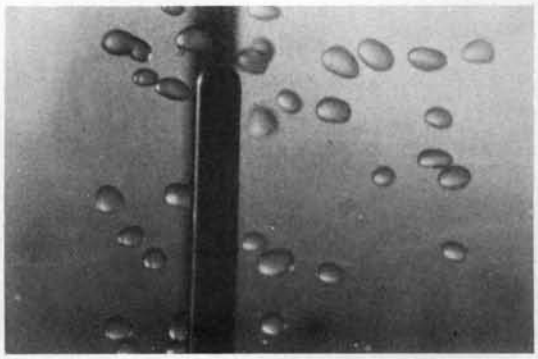

b

Q_d = 6.67 cc./s.

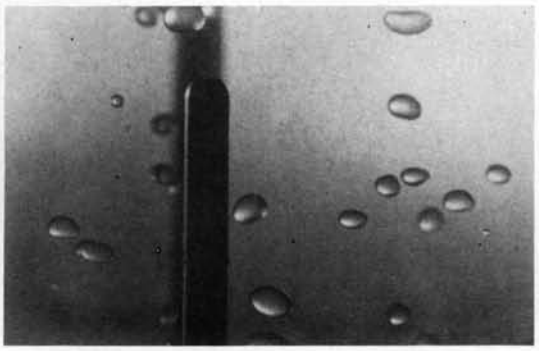

c

Q_d = 5.03 cc./s.

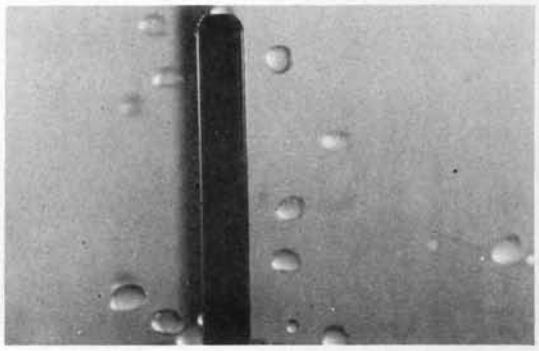

d

Q_d = 3.37 cc./s.

Figure 5 Photographs of drops sizes with varying flow rates of dispersed phase (distributor B)

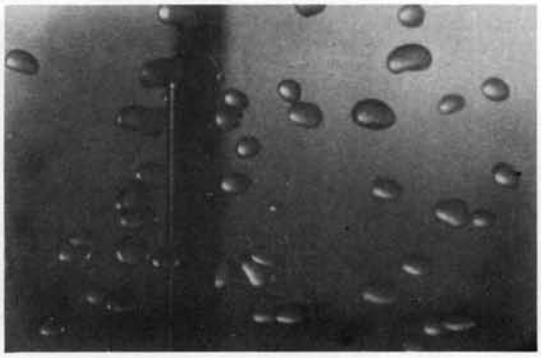

a

Q_d = 8.68 cc./s.

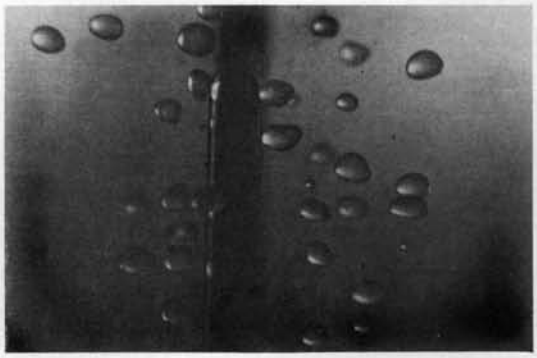

b

Q_d = 6.67 cc./s.

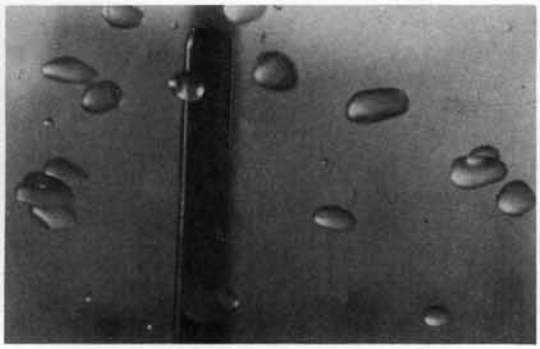

c

Q_d = 5.03 cc./s.

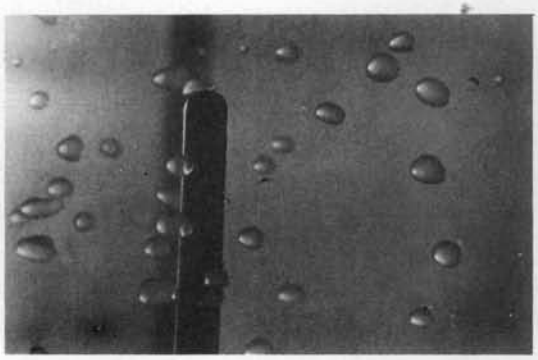

d

Q_d = 3.37 cc./s.

Figure 6 Photographs of drops sizes with varying flow rates of dispersed phase (distributor C)

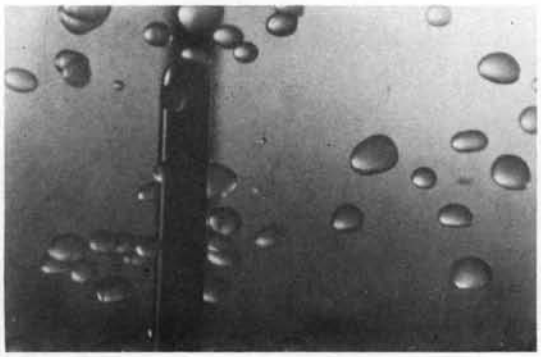

a

Q_d = 8.68 cc./s.

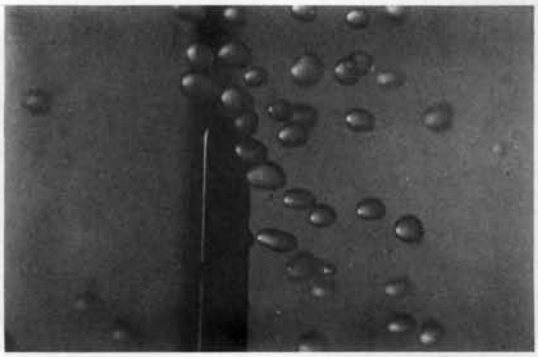

b

Q_d = 6.67 cc./s.

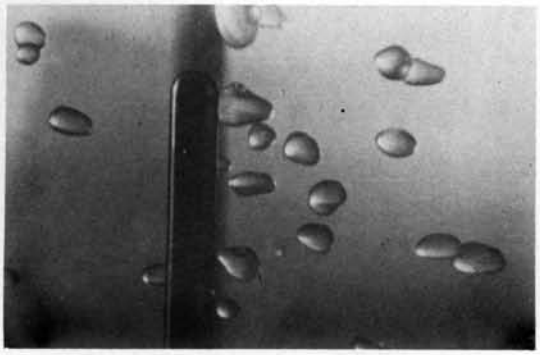

c

Q_d = 5.03 cc./s.

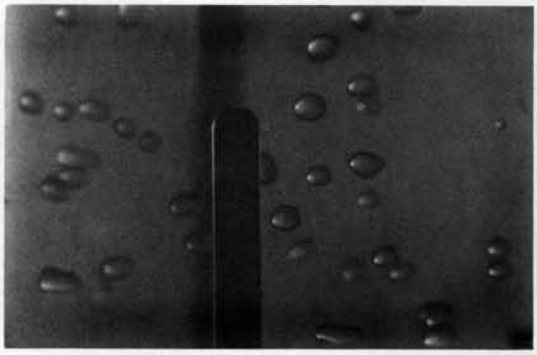

d

Q_d = 3.37 cc./s.

Figure 7 Photographs of drops sizes with varying flow rates of dispersed phase (distributor D)

a

Q_d = 8.68 cc./s.

b

Q_d = 6.67 cc./s.

c

Q_d = 5.03 cc./s.

Figure 8 Long time exposure of drops
(to calculate local velocities)
- distributor A

a

Q_d = 8.68 cc./s.

b

Q_d = 6.67 cc./s.

c

Q_d = 5.03 cc./s.

Figure 9 Long time exposure of drops
(to calculate local velocities)
- distributor B

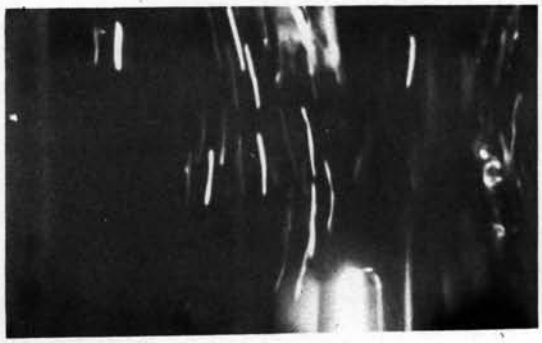

a

Q_d = 8.68 cc./s.

b

Q_d = 6.67 cc./s.

c

Q_d = 5.03 cc./s.

Figure 10 Long time exposure of drops
(to calculate local velocities)
- distributor C

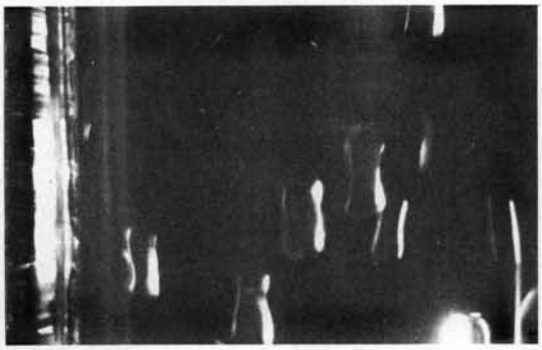

a

Q_d = 8.68 cc./s.

b

Q_d = 6.67 cc./s.

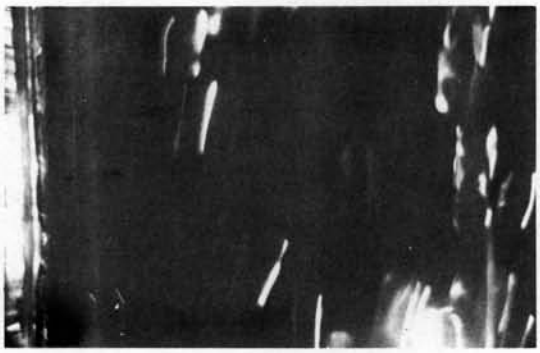

c

Q_d = 5.03 cc./s.

Figure 11 Long time exposure of drops
(to calculate local velocities)
- distributor D

$$V_F = \frac{4}{3} \P d_1 d_2^2 \qquad (10)$$

From this volume the droplet diameter can be obtained from the equation.

$$d_F = \left(\frac{3V_F}{4\P}\right)^{1/3} \qquad (11)$$

The average drop size was obtained from drop size at maximum size frequency.

The method to obtaining the velocity profile of drops used measurements of length and angles of direction of drop fall both of which were measured from a screen. The screen was divided into several vertical sections each respresenting a 2.0 mm. radical section of the column. In each section drops were found to have varying velocities. These velocities were then averaged for each radial section to enable a radial profile of drop velocities to be made.

3.2 Results

As can be seen from the equations given in the literature review section the most important parameters that must be used to predict drop diameters, drop size distributions and velocities of drops are the nozzle diameter and the nozzle velocity. These parameters were available from the experimental data. Drop sizes were evaluated from equation 1 to 7, drop size distributions and velocities of drop were plotted using the experimental data, hold-up could be calculated from equation 9. The results of drop size, drop size distributions, velocities of drop are as follow:

3.2.1 Drop size

Equation 1 to 7 were used to calculate drop sizes for all four distributor types and all four flow rates. The jetting velocity v_j was calculated from equation 8. Table 3 to 6 showed the comparison of predicted drop size equation with experimental data for four sets of distributors. A mean absolute error of 8.70% was found when predicting drop sizes from equation 5 of Skelland and Johnson, 20.63% for equation 2 of Horvath et al., 26.80% for equation 1 of Vediayan et al., and 52.08% for equation 6 of Hayworth and Treybal. Experimental and calculated values of drop size are represented in figures 12 to 15 as a function of nozzle velocity. From these figures it can be seen that the calculated drop sizes predicted by Skelland and Johnson compare well with the experimental results, and those predicted by Horvath et al., and Vedaiyan et al. correlate also well with the experimental results.

3.2.2 Drop size distribution

Figures 16 to 19 show the drop size distributions for an average nozzle velocity of 11.63 cm/s (flow rate = 3.37 cm/s). The distribution remains monomodal with little deviations except in the case of distributor C which yields a trimodal set of data and distributor D which yields a bimodal set of data. In figures 20 to 23 the average nozzle velocity is 17.35 cm/s (flow rate = 5.03 cc/s), the distribution yields a bimodal set of data. In figures 24 to 27 the average nozzle velocity is 23.00 cm/s (flow rate = 6.67 cc/s)

Table 3 Comparison of predicted drop size equation with experimental data for distributor A.

Flow rates of dispersed phases (cc/s)	Diameter of drops from distributor A (mm.)										
	d_{op}	d_{43}	d_{32}	d_F from Equation (5)	% error from d_{32} using Equation (5)	d_F from Equation (2)	% error from d_{32} using Equation (2)	d_F from Equation (1)	% error from d_{32} using Equation (1)	d_F from Equation (6)	% error from d_{32} using Equation (6)
8.68	2.35	2.60	2.55	2.78	+ 9.02	2.86	+12.16	4.13	+61.96	1.19	-53.53
6.67	2.65	2.81	2.76	2.98	+ 7.97	3.30	+10.74	4.28	+55.07	1.39	-49.64
5.03	2.95	2.99	2.96	3.05	+ 3.04	4.10	+34.43	4.55	+50.34	1.60	-45.95
3.37	3.45	3.41	3.39	3.16	- 5.90	6.01	+90.19	4.69	+38.35	1.86	-45.13

Table 4 Comparison of predicted drop size equation with experimental data for distributor B.

Flow rates of dispersed phases (cc/s)	Diameter of drops from distributor B (mm.)										
	d_{op}	d_{43}	d_{32}	d_F from Equation (5)	% error from d_{32} using Equation (5)	d_F from Equation (2)	% error from d_{32} using Equation (2)	d_F from Equation (1)	% error from d_{32} using Equation (1)	d_F from Equation (6)	% error from d_{32} using Equation (6)
8.68	2.85	2.99	2.97	3.60	+21.21	3.17	+ 6.73	4.18	+40.74	1.31	-55.89
6.67	3.00	3.13	3.07	3.57	+16.29	3.38	+10.10	4.33	+41.04	1.53	-50.16
5.03	3.20	3.44	3.38	3.61	+ 6.80	3.87	+14.50	4.50	+24.89	1.75	-48.22
3.37	4.00	3.98	3.92	3.73	- 4.85	5.25	+33.93	4.75	+21.17	1.93	-50.77

Table 5 Comparison of predicted drop size equation with experimental data for distributor C.

Flow rates of dispersed phase (cc/s)	Diameter of drops from distributor C (mm.)										
	d_{op}	d_{43}	d_{32}	d_F from Equation (5)	% error from d_{32} using Equation (5)	d_F from Equation (2)	% error from d_{32} using Equation (2)	d_F from Equation (1)	% error from d_{32} using Equation (1)	d_F from Equation (6)	% error from d_{32} using Equation (6)
8.68	3.40	3.74	3.67	4.10	+11.72	3.37	- 8.17	4.27	+16.35	1.50	-59.13
6.67	3.10	3.85	3.77	3.84	+ 1.86	3.35	-11.14	4.42	+17.24	1.73	-54.11
5.03	3.30	3.79	3.70	3.78	+ 2.16	3.54	- 4.32	4.59	+24.05	1.96	-47.03
3.37	4.10	4.08	4.02	3.85	- 4.23	4.33	+ 7.71	4.84	+20.40	2.14	-46.77

Table 6 Comparison of predicted drop size equation with experimental data for distributor D.

Flow rates of dispersed phases (cc/s)	Diameter of drops from distributor D (mm.)										
	d_{op}	d_{43}	d_{32}	d_F from Equation (5)	% error from d_{32} using Equation (5)	d_F from Equation (2)	% error from d_{32} using Equation (2)	d_F from Equation (1)	% error from d_{32} using Equation (1)	d_F from Equation (6)	% error from d_{32} using Equation (6)
8.68	4.60	4.66	4.59	5.31	+15.69	3.71	-19.17	4.30	- 6.32	1.60	-65.14
6.67	4.10	4.45	4.38	4.39	+ 0.23	3.48	-20.55	4.45	+ 1.60	1.85	-57.76
5.03	4.20	4.59	4.52	3.97	-12.17	3.38	-25.22	4.62	+ 2.21	2.07	-54.20
3.37	4.30	4.64	4.56	3.83	-16.01	3.60	-21.05	4.88	+ 7.02	2.28	-50.00

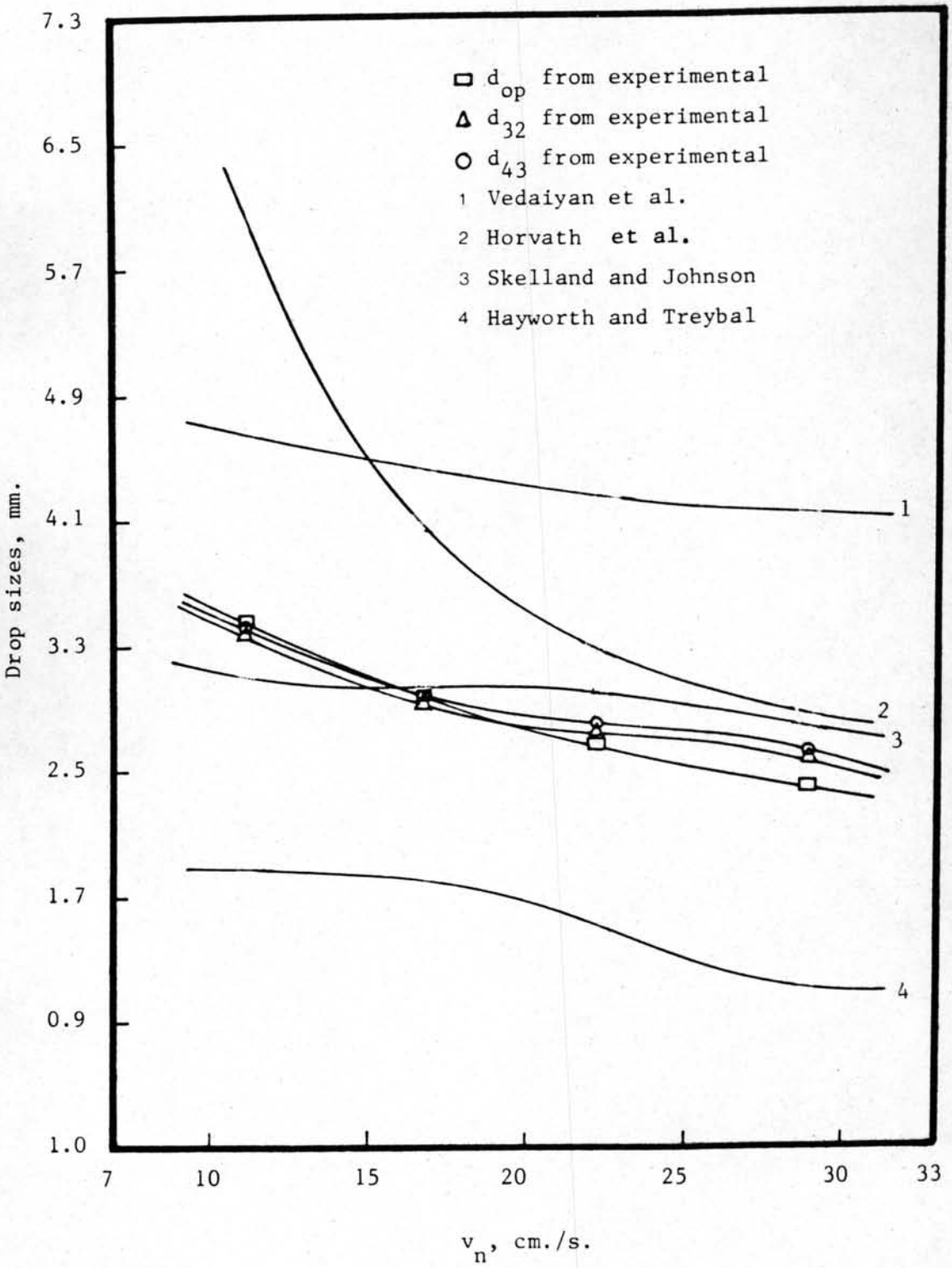

Figure 12 Drop size as a function of nozzle velocity (distributor A)

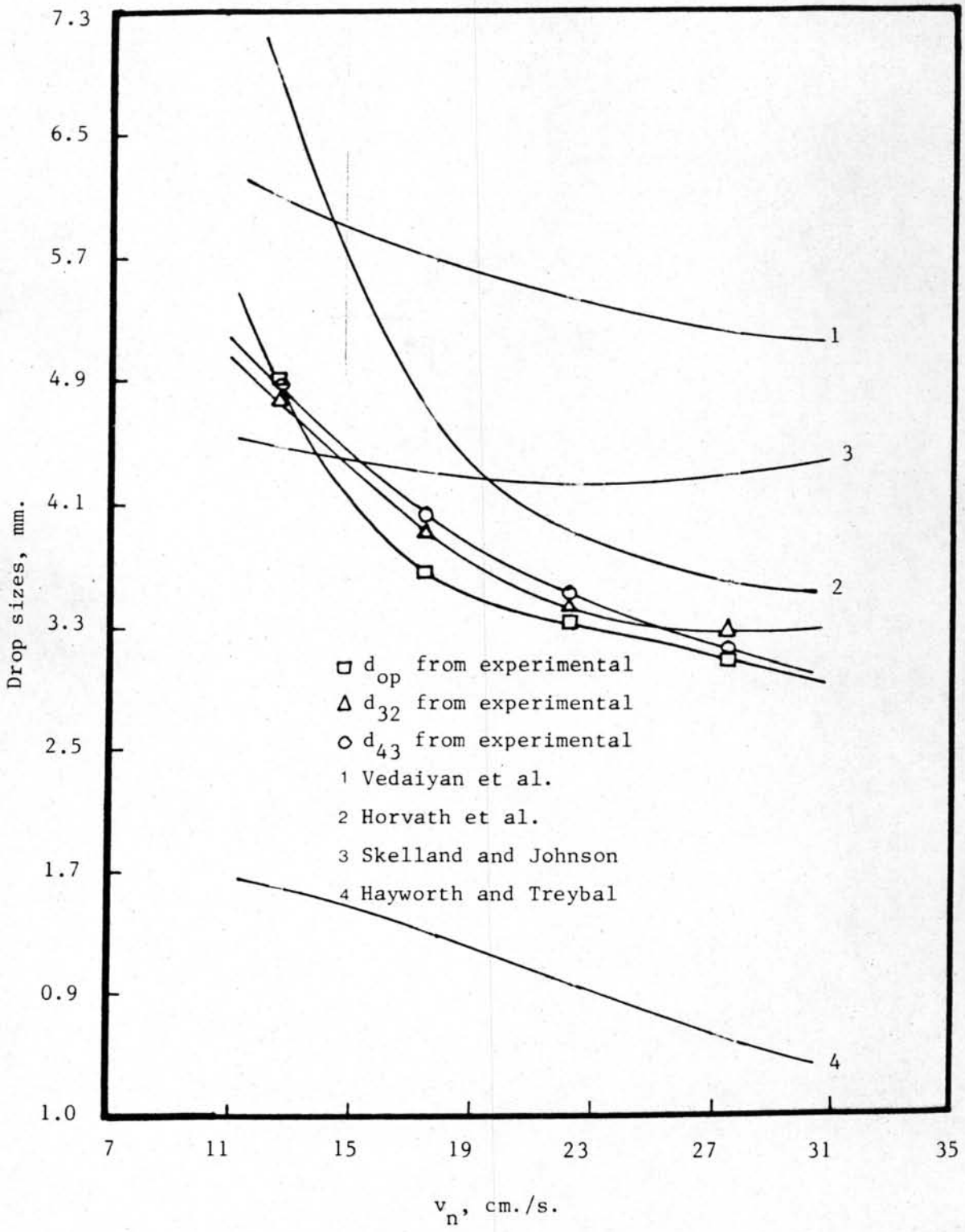

Figure 13 Drop size as a function of nozzle velocity (distributor B)

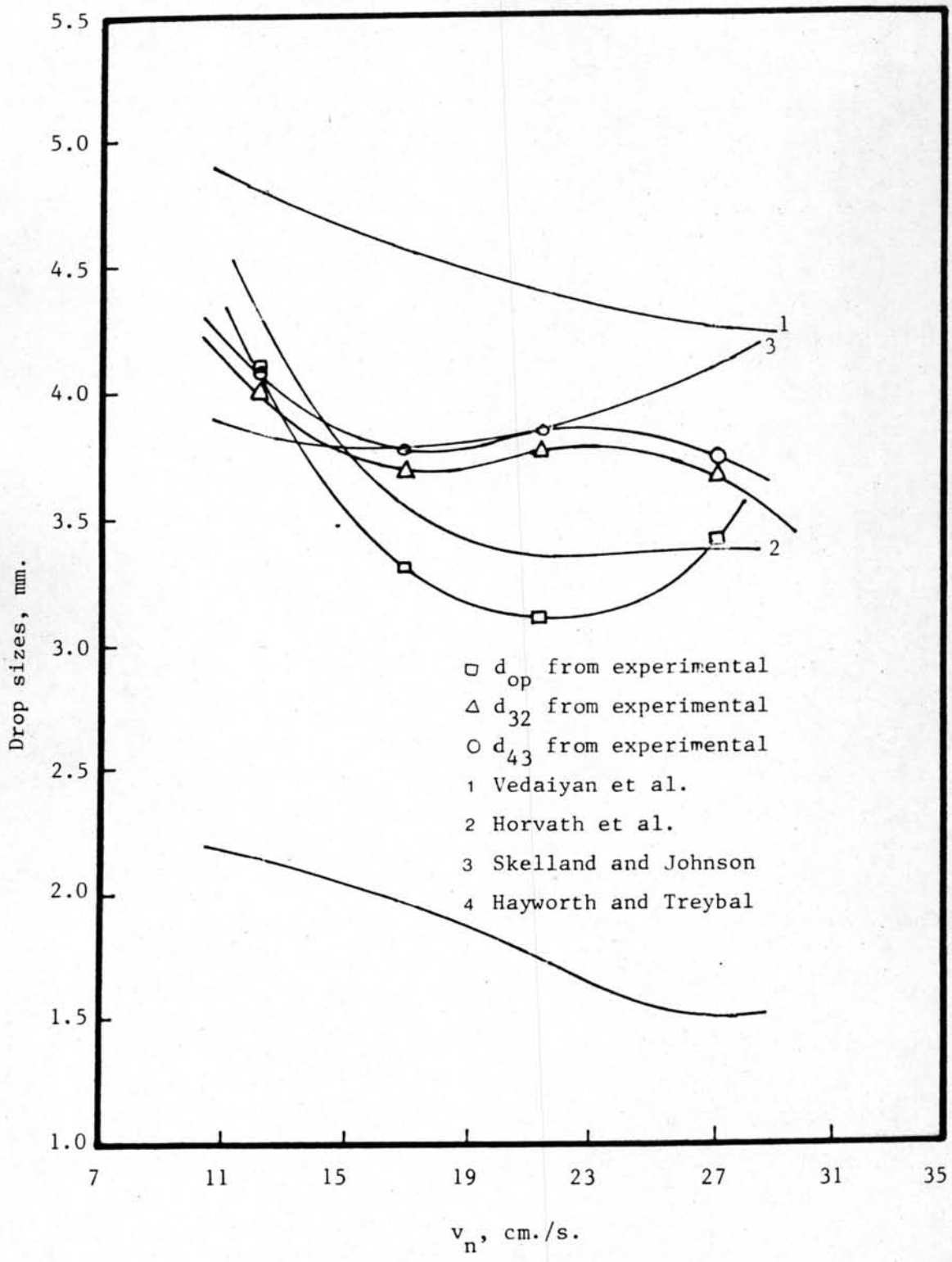

Figure 14 Drop size as a function of nozzle velocity (distributor C)

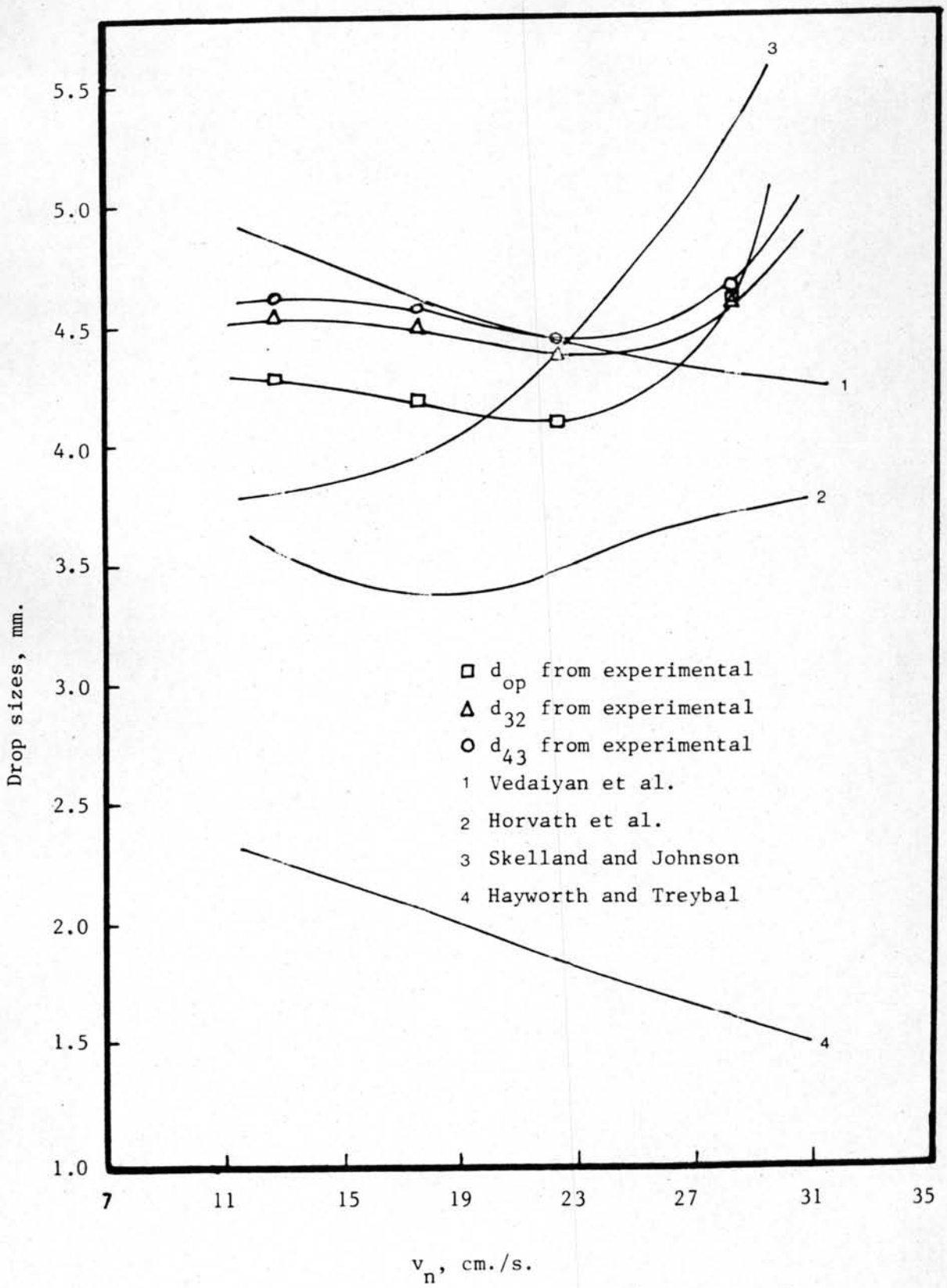

Figure 15 Drop size as a function of nozzle velocity (distributor D)

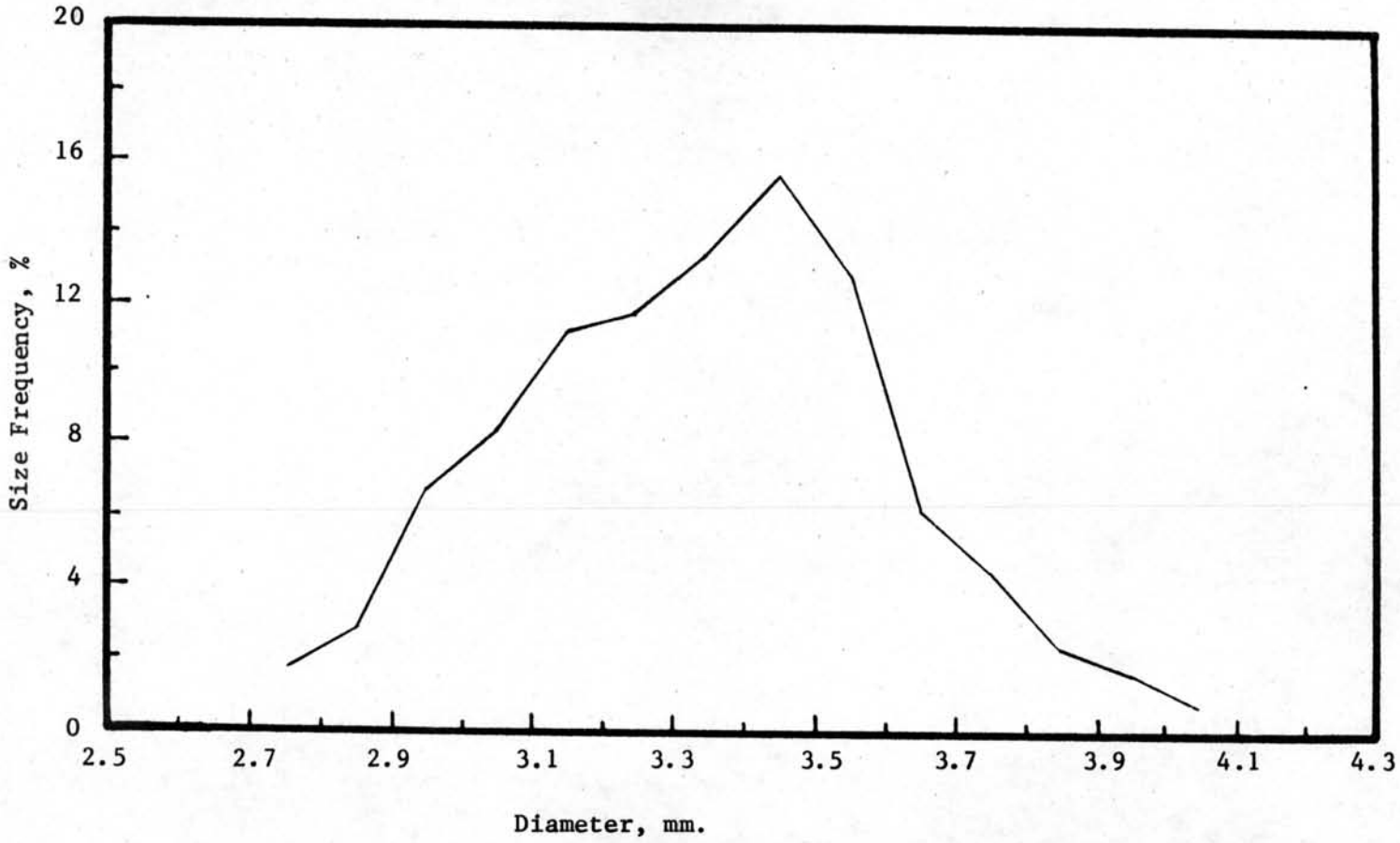

Figure 16 Drop size distribution (distributor A flow rate 3.37 cc./s.)

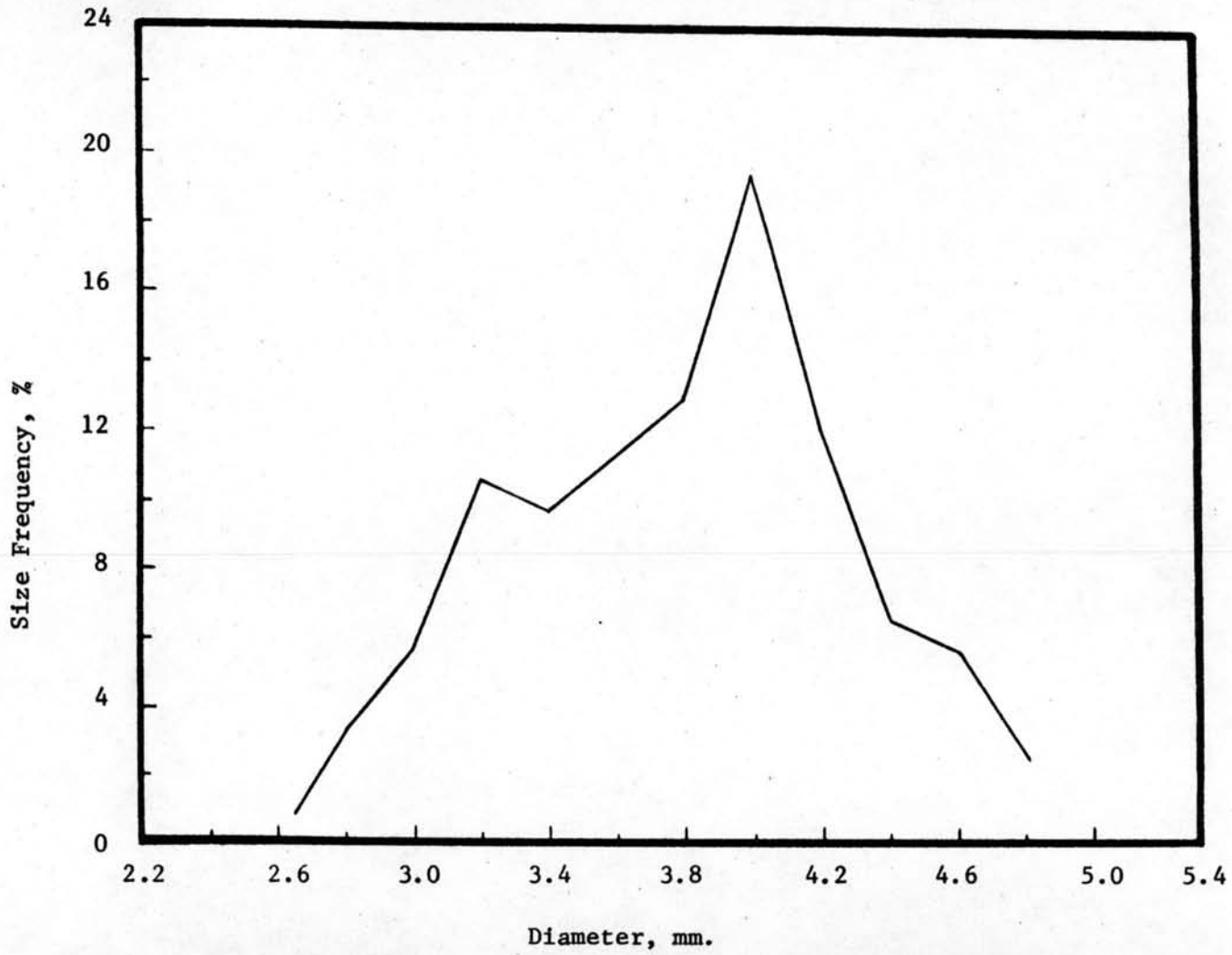

Figure 17 Drop size distribution (distributor B flow rate 3.37 cc./s.)

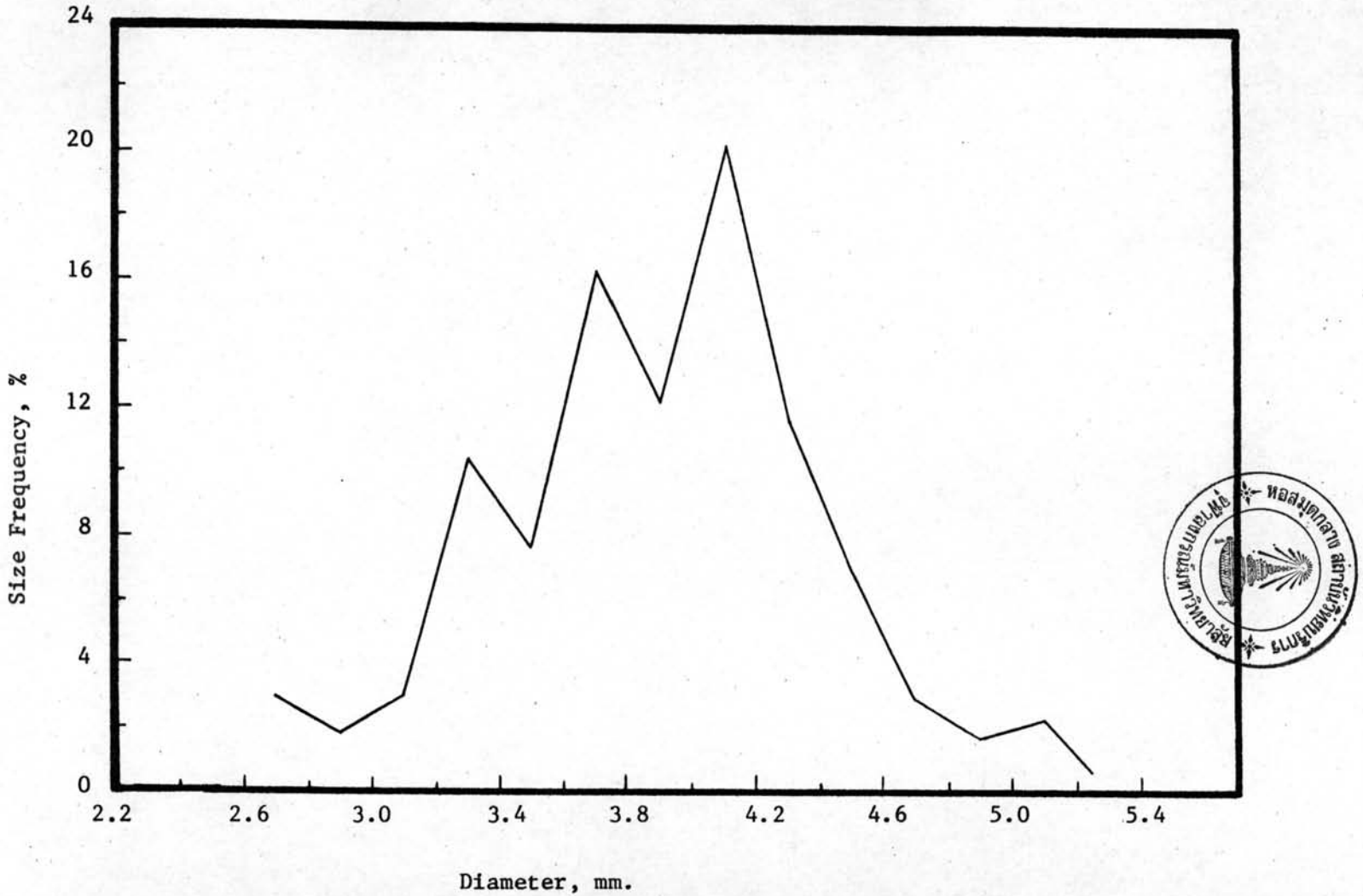

Figure 18 Drops size distribution (distributor C flow rate 3.37 cc./s.)

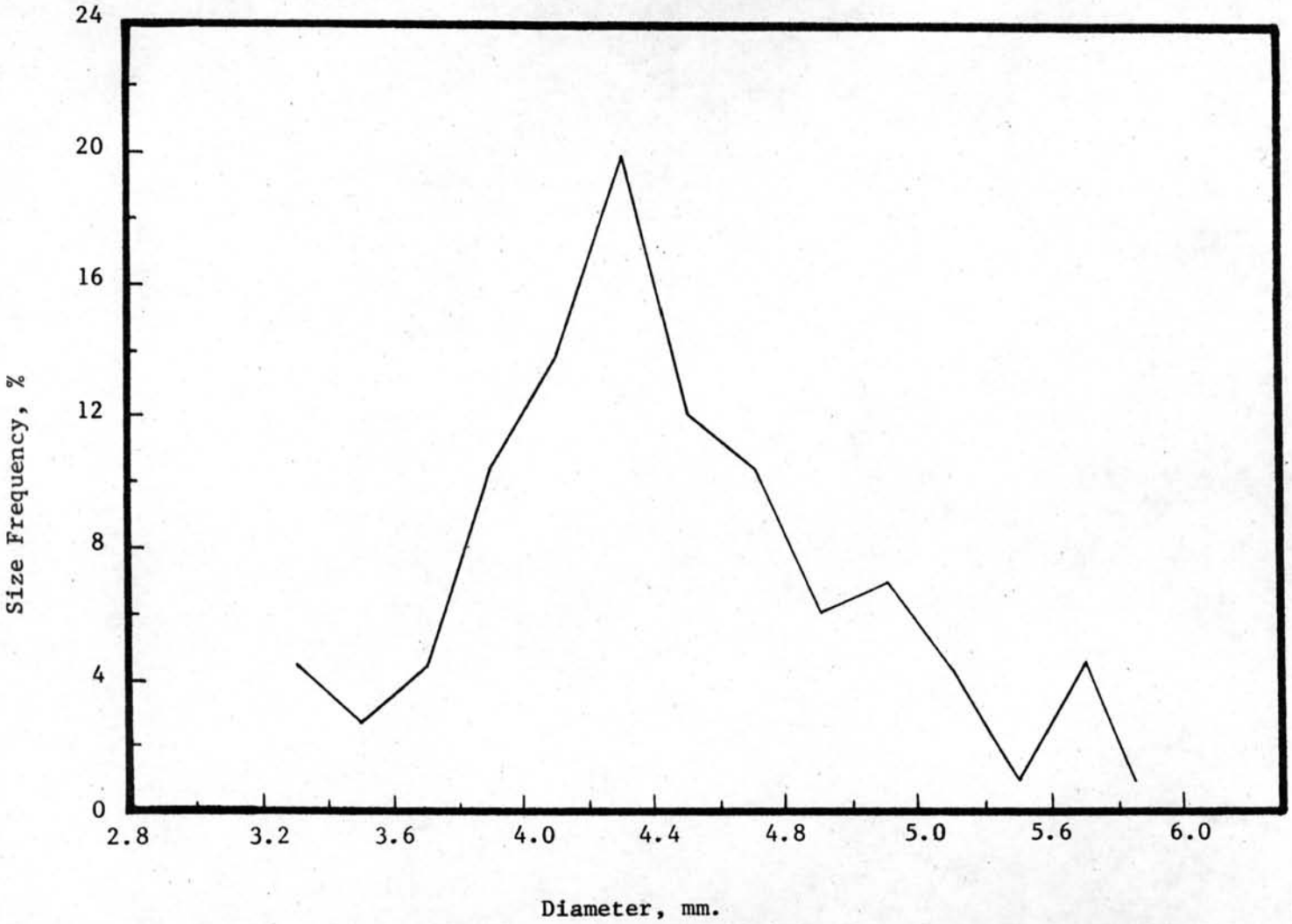

Figure 19 Drops size distribution (distributor D flow rate 3.37 cc./s.)

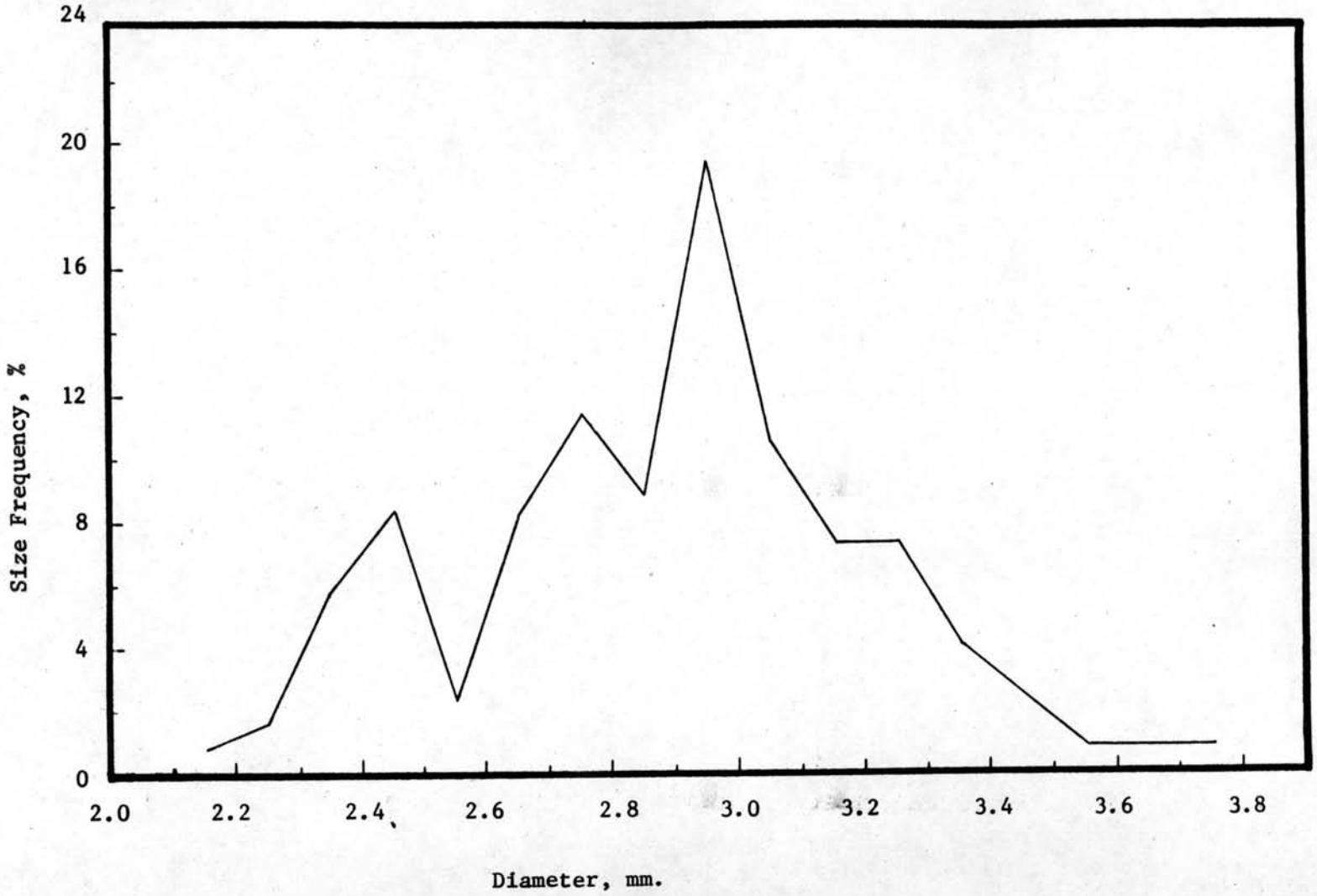

Figure 20 Drops size distribution (distributor A flow rate 5.03 cc./s.)

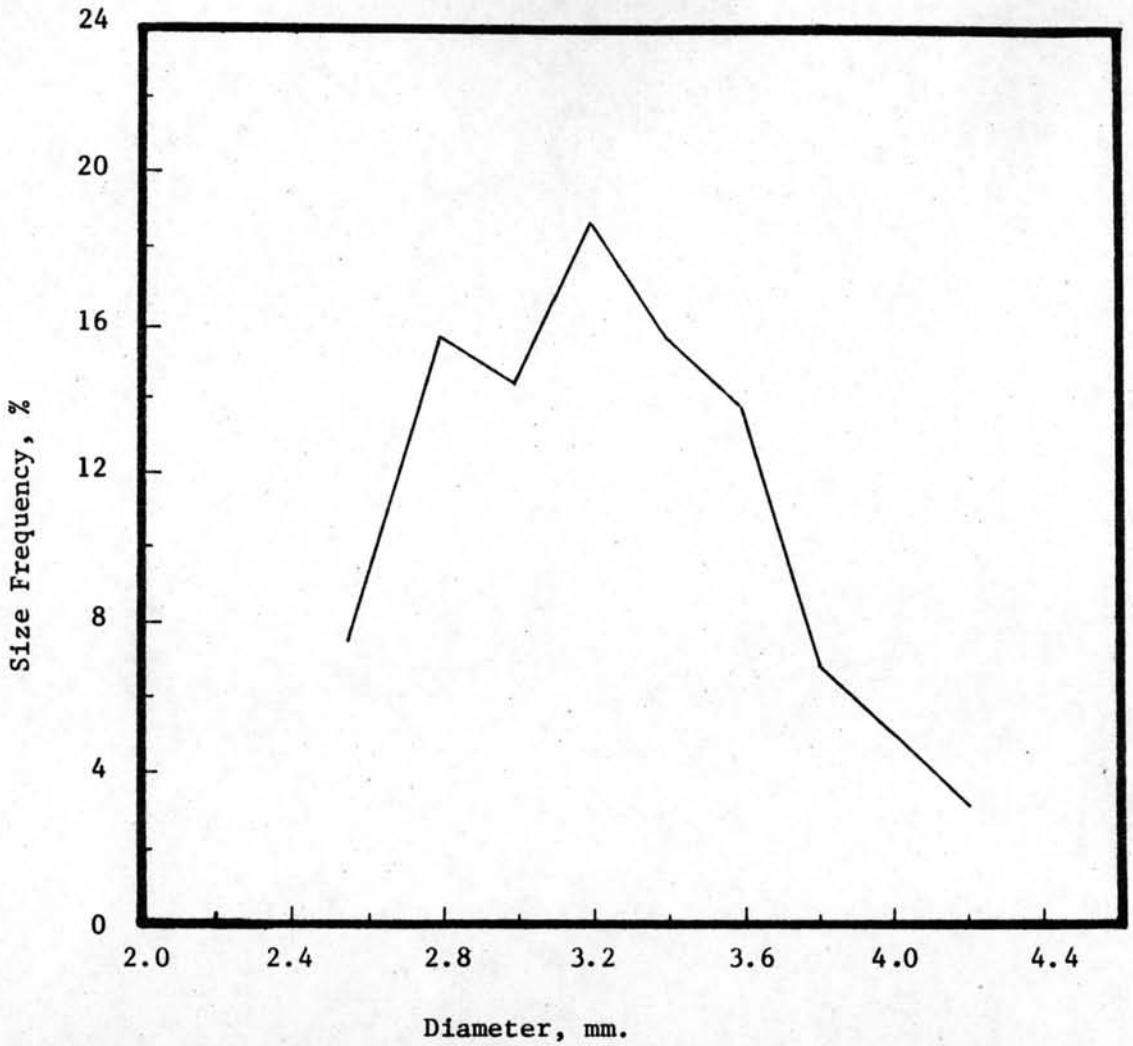

Figure 21 Drops size distribution (distributor B flow rate 5.03 cc./s.)

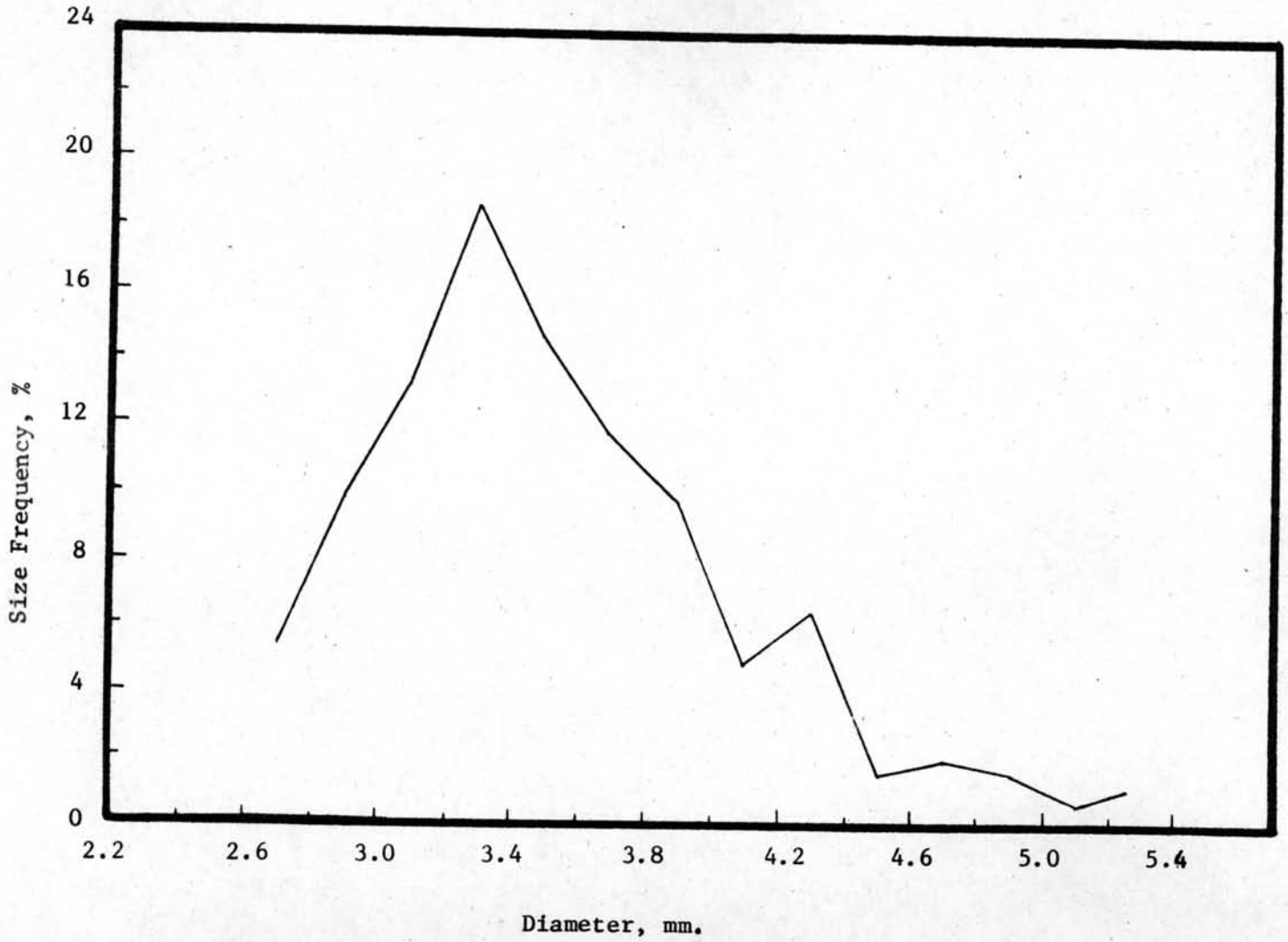

Figure 22 Drops size distribution (distributor C flow rate 5.03 cc./s.)

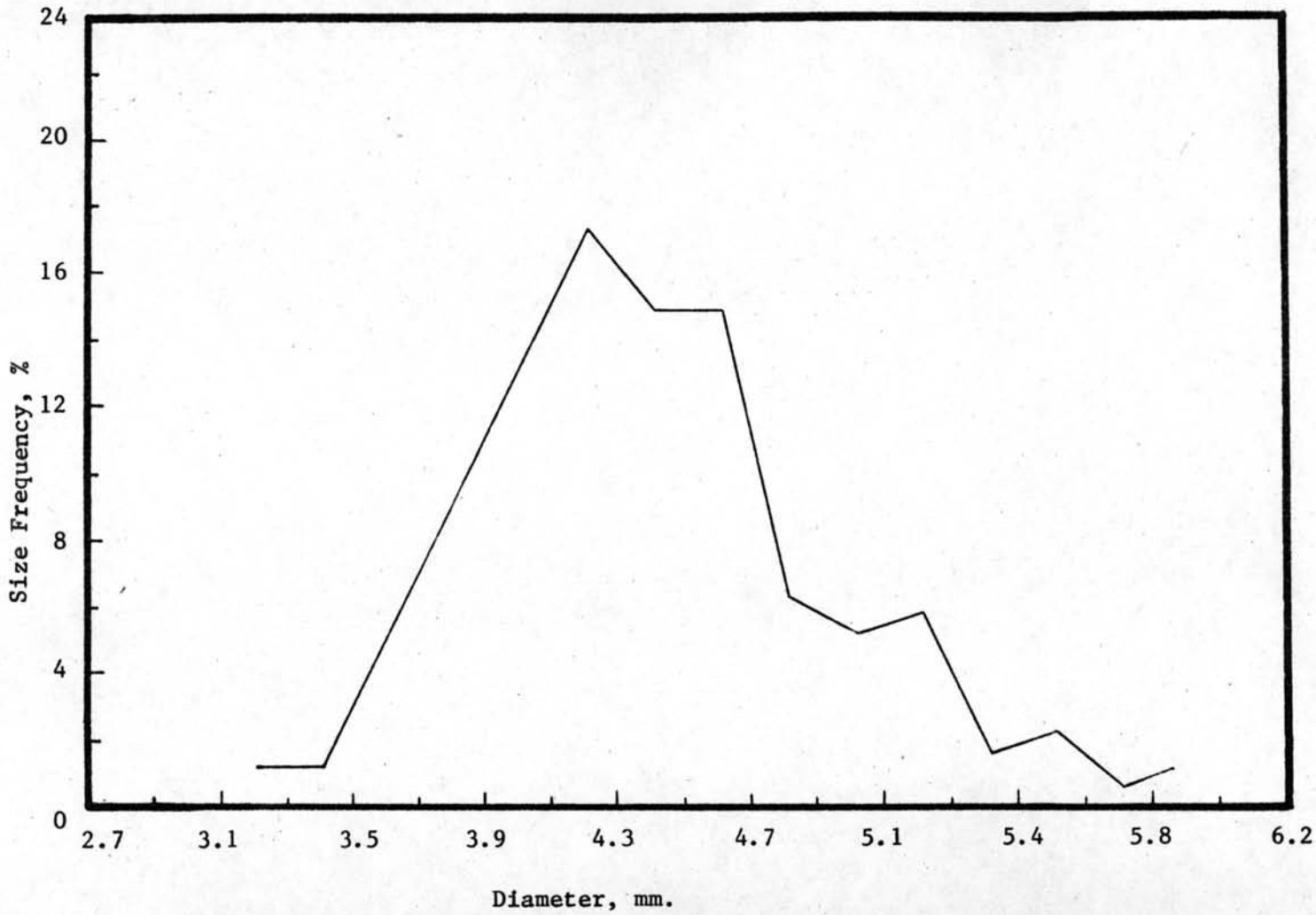

Figure 23 Drops size distribution (distributor D flow rate 5.03 cc./s.)

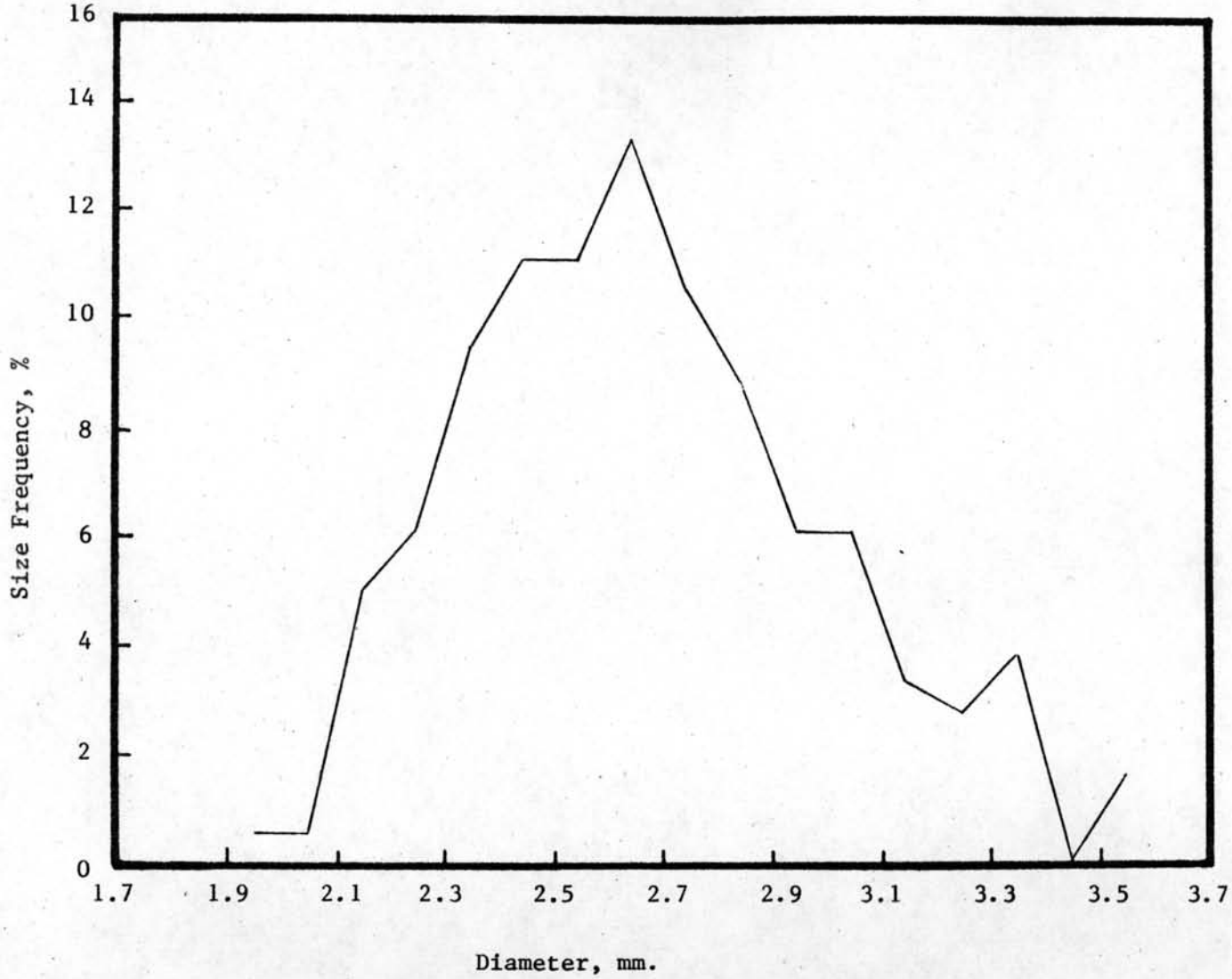

Figure 24 Drops size distribution (distributor A flow rate 6.67 cc./s.)

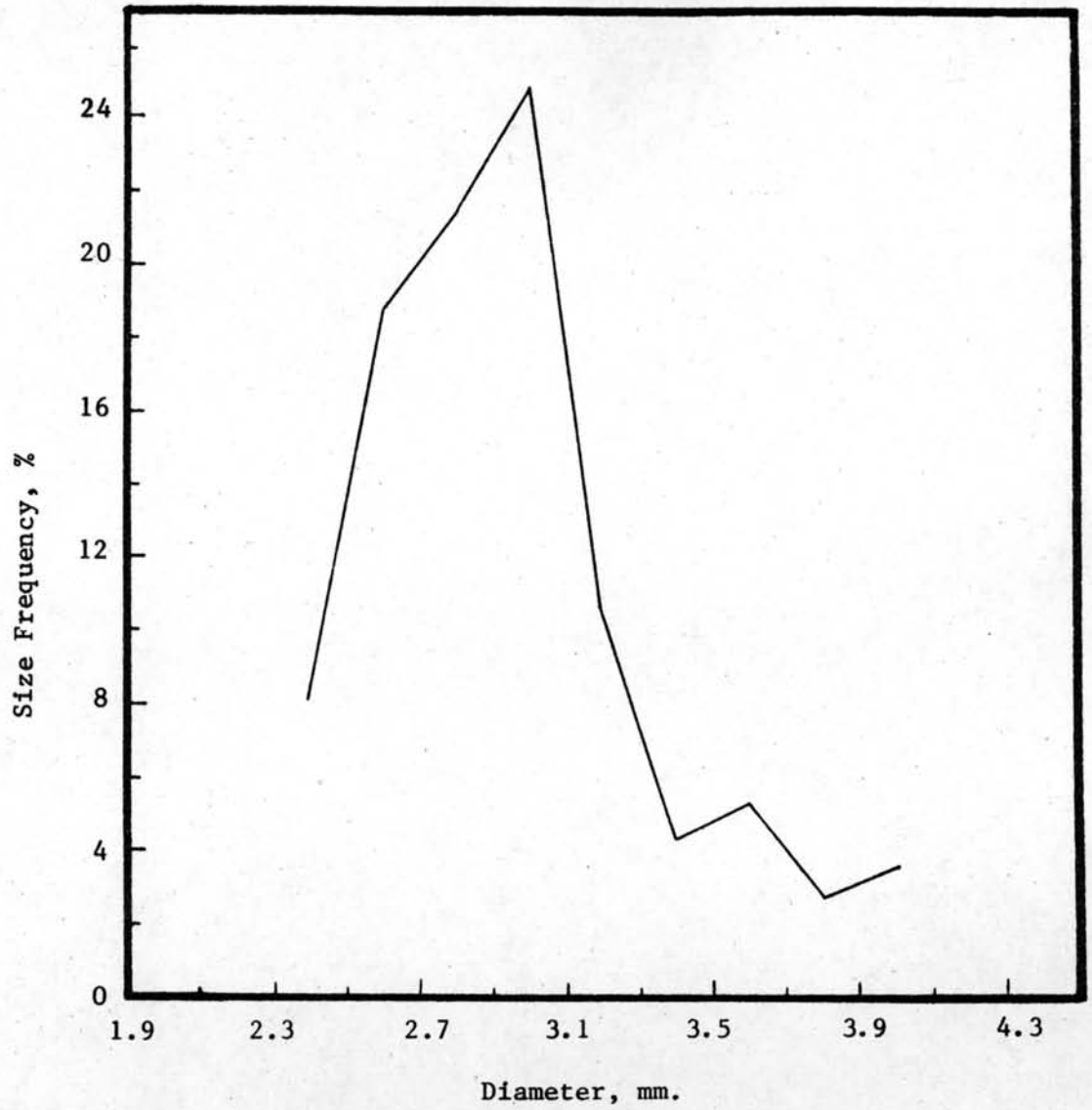

Figure 25 Drops size distribution (distributor B flow rate 6.67 cc./s.)

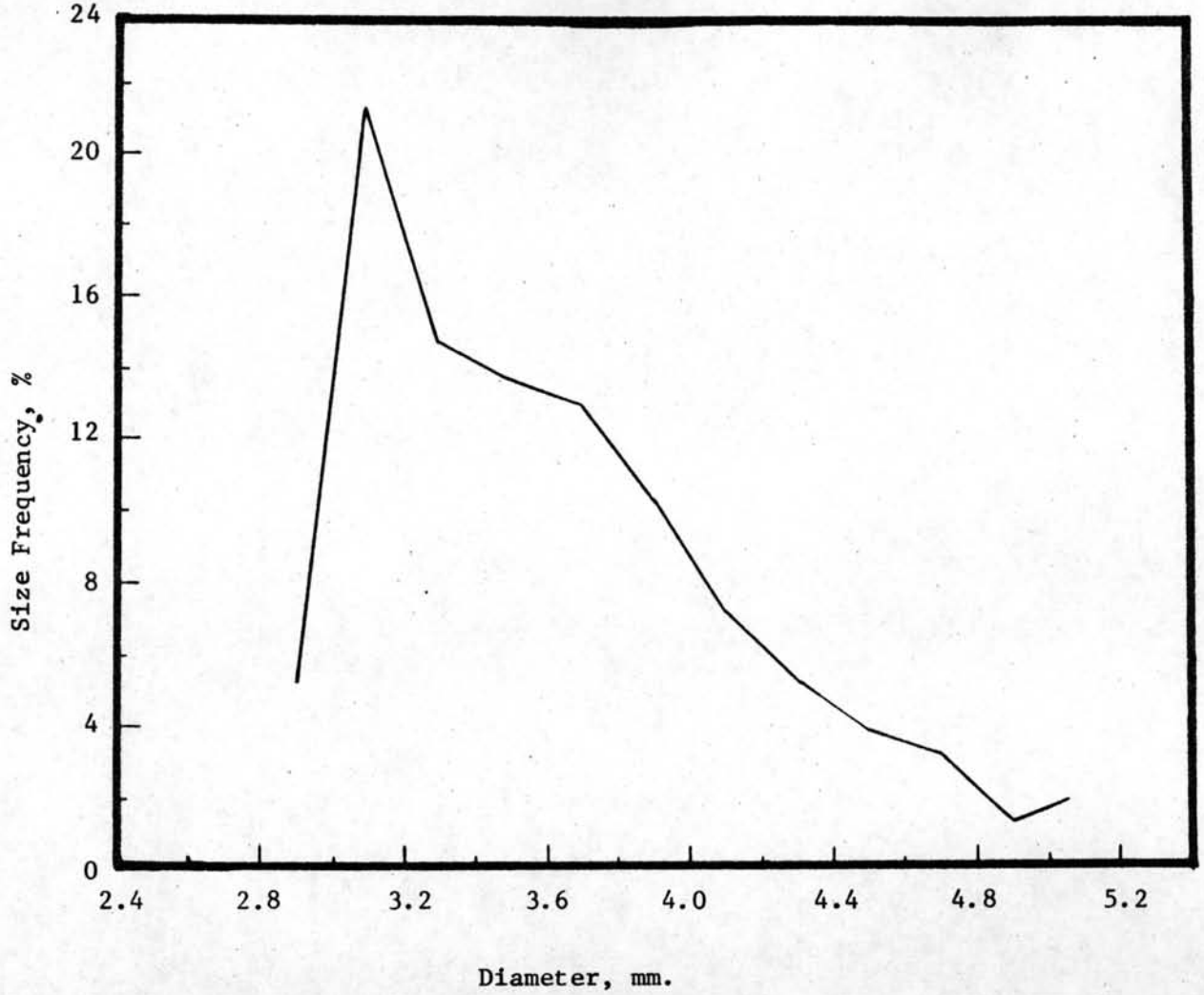

Figure 26 Drops size distribution (distributor C flow rate 6.67 cc./s.)

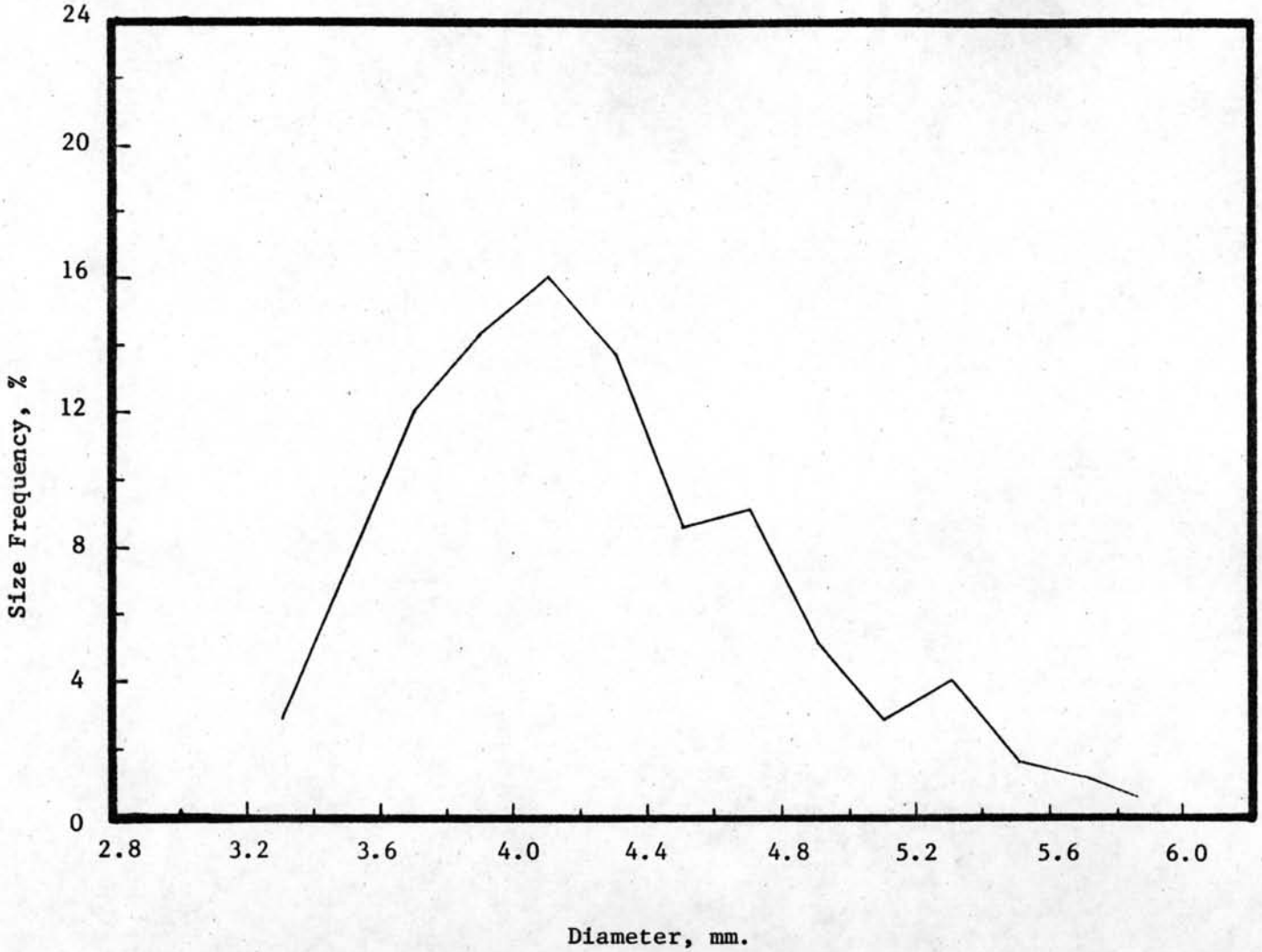

Figure 27 Drops size distribution (distributor D flow rate 6.67 cc./s.)

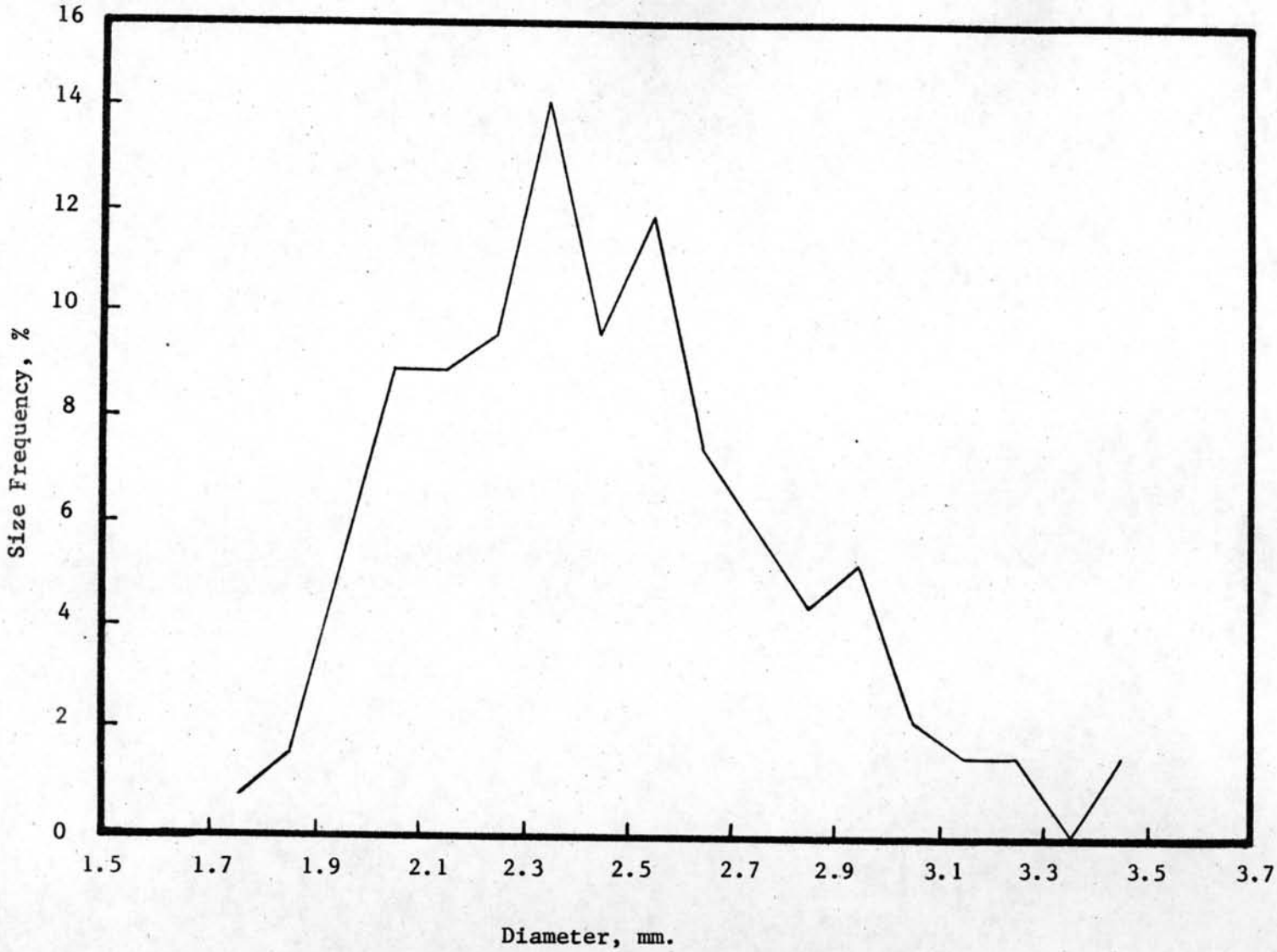

Figure 28 Drops size distribution (distributor A flow rate 8.68 cc./s.)

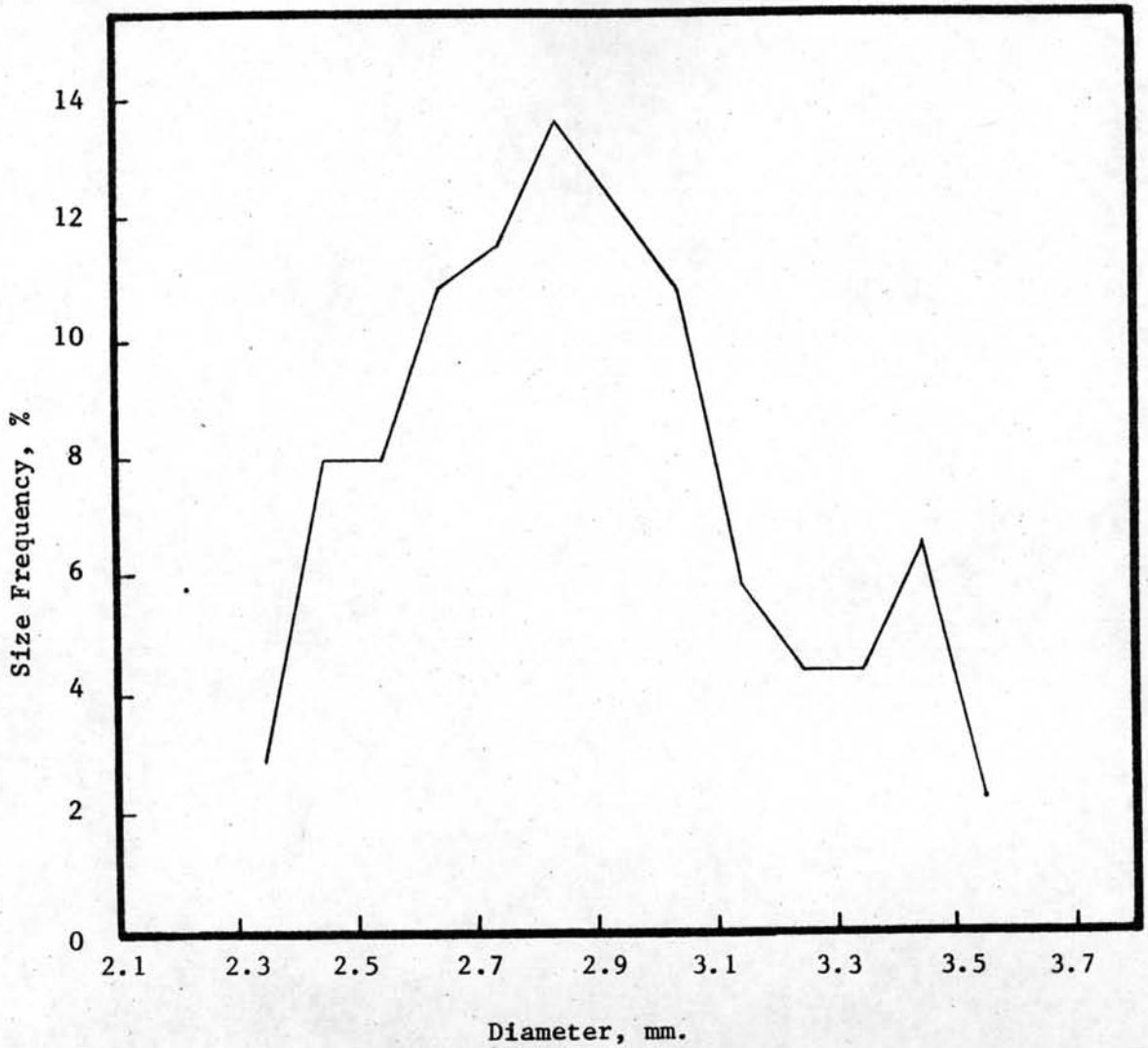

Figure 29 Drops size distribution (distributor B flow rate 8.68 cc./s.)

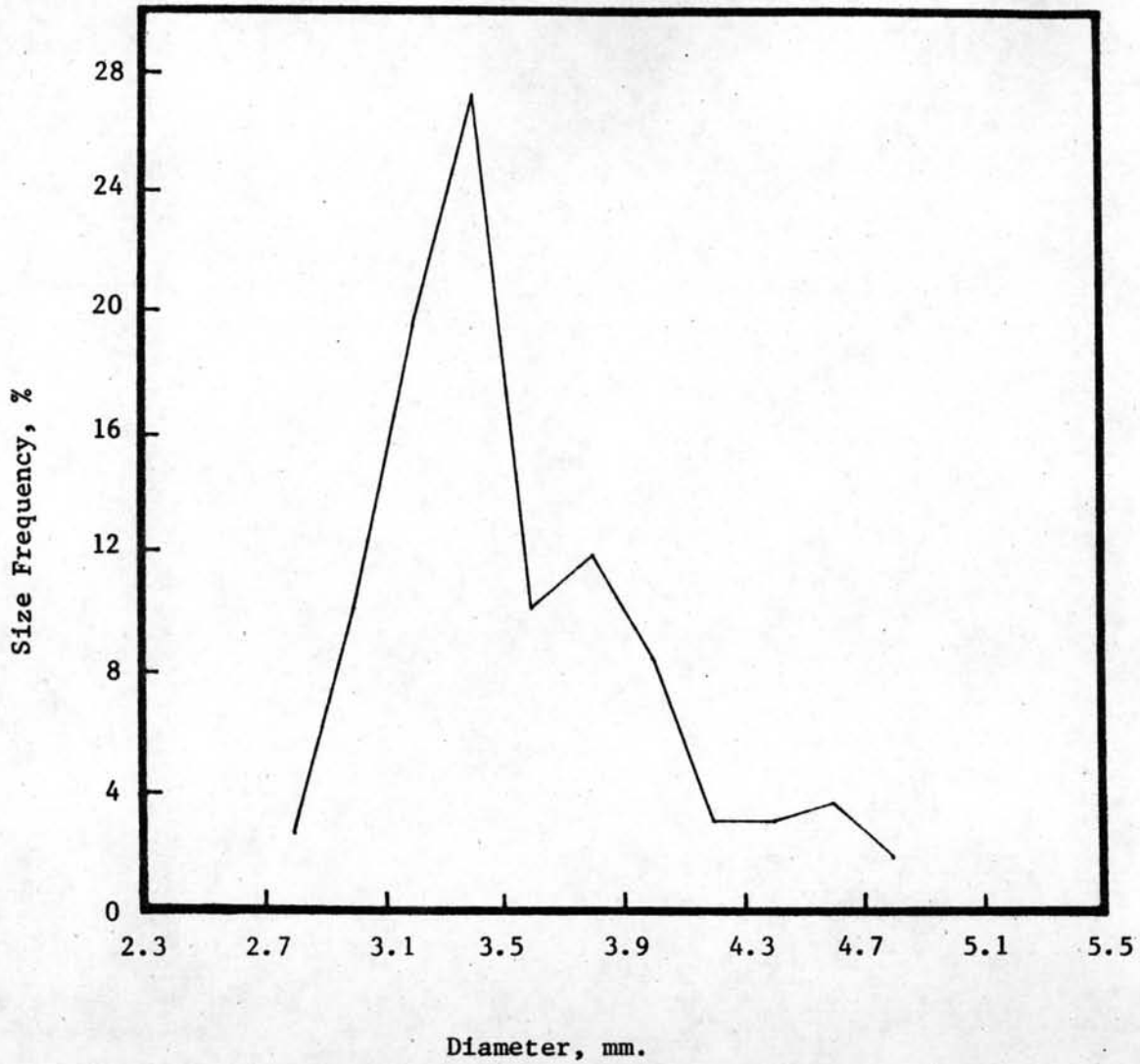

Figure 30 Drops size distribution (distributor C flow rate 8.68 cc./s.)

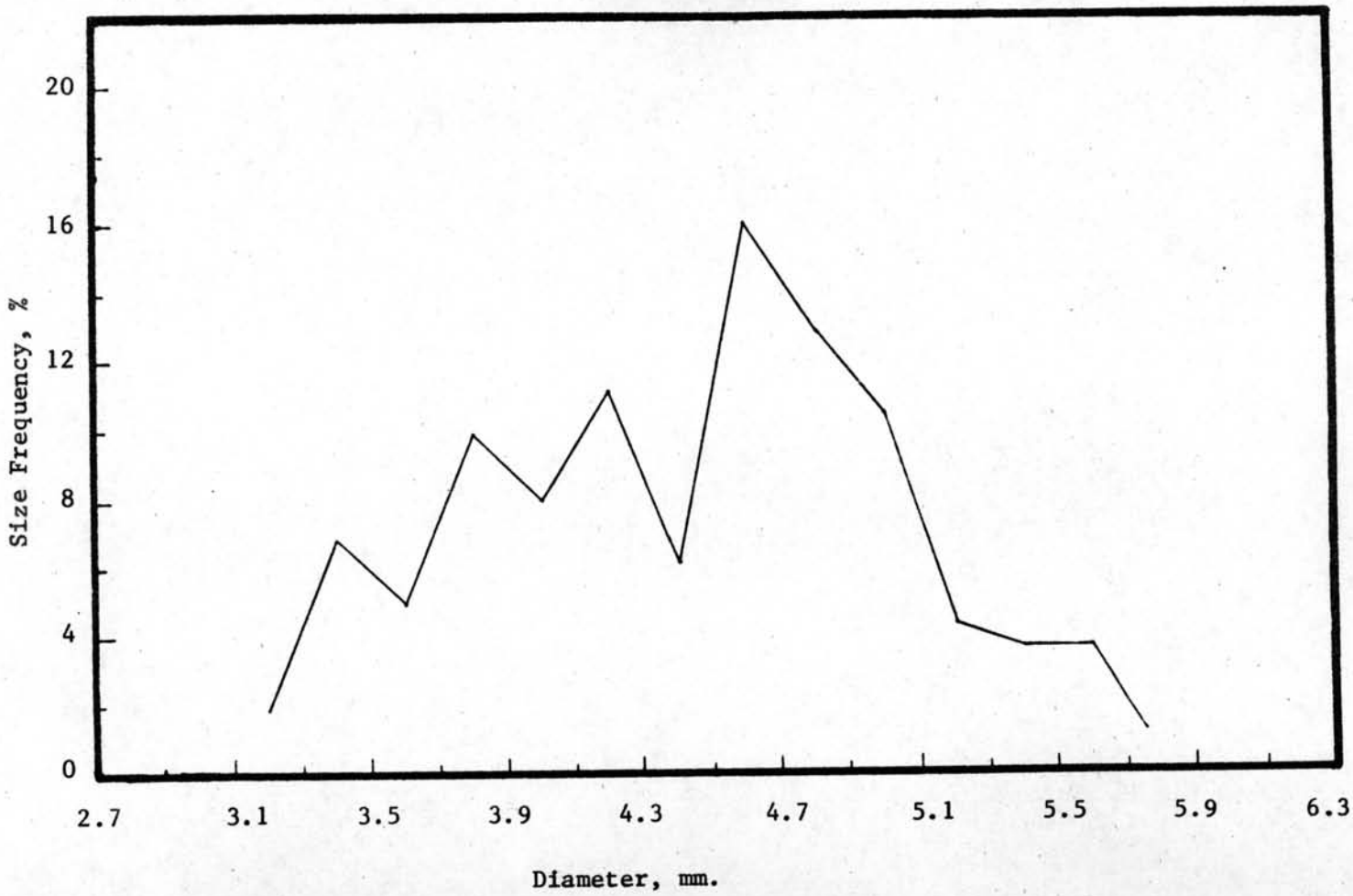

Figure 31 Drops size distribution (distributor D flow rate 8.68 cc./s.)

and in figures 28 to 31 the average nozzle velocity is 29.94 cm/s (flow rate = 8.68 /s), the distribution curves become bimodal and trimodal except in the case of distribution D which at a nozzle velocity of 29.94 cm/s has a tetramodal set of data. For these results it is believed that these size distribution curves are resonable compared to Vedaiyan et al. and Horvath et al. experiments.

3.3.3 Velocity of drop

Figures 32 to 43 show the experimentally determined velocity profiles of drops and the calculated terminal velocities of drop. Terminal velocities can be calculated from Hu & Kinter's equation[14] and Vigne's equation[15]

Hu & Kinter's equation:

$$R_e \cdot P^{-0.15} < 8 \; ; \; C_D = 2.5 \, R_e W_e^{-1} P^{-0.30}$$

$$R_e \cdot P^{-0.15} > 8 \; ; \; C_D = 5 W_e^{-1} P^{-0.15} \, (R_e P^{-0.15} - 4)$$

when $$R_e = \frac{d_F \rho_c V_t}{\mu}$$

$$P = \frac{\rho_c^2 \gamma^3}{g \Delta\rho \mu^4}$$

$$C_D = \frac{4}{3} \frac{g \Delta\rho d_F}{\rho_c V_t^2}$$

Vigne's equation:

$$1 < R_e < 1000; \; V_t = \frac{d_F}{4.2} \left(\frac{g\Delta\rho}{\rho_c} \right)^{2/3} \left(\frac{\rho_c}{\mu c} \right)^{1/3} \left(1 - \frac{g \Delta\rho d_F^2}{6\gamma} \right)$$

The velocity profiles of drops are paraboloidal in shape except in the case of distributor A for flow rates 8.68, 6.67 cc/s and in the case of distributor B for a flow rate of 8.68 cc.s. The equations representing these velocity profiles are show in table 7.

Table 7 Equations representing velocity profiles of drop.

No.	Distributor	Flow rate cc/s	Equations representing velocity profiles of drop
1	A	5.03	$y = 1.54x^{1.32}$
2	B	6.67	$y = 1.94x^{1.27}$
3	B	5.03	$y = 1.38x^{1.47}$
4	C	8.68	$y = 1.48x^{1.30}$
5	C	6.67	$y = 1.39x^{1.46}$
6	C	5.03	$y = 0.12x^{2.98}$
7	D	8.68	$y = 0.15x^{2.70}$
8	D	6.67	$y = 0.13x^{2.58}$
9	D	5.03	$y = 0.39x^{1.90}$

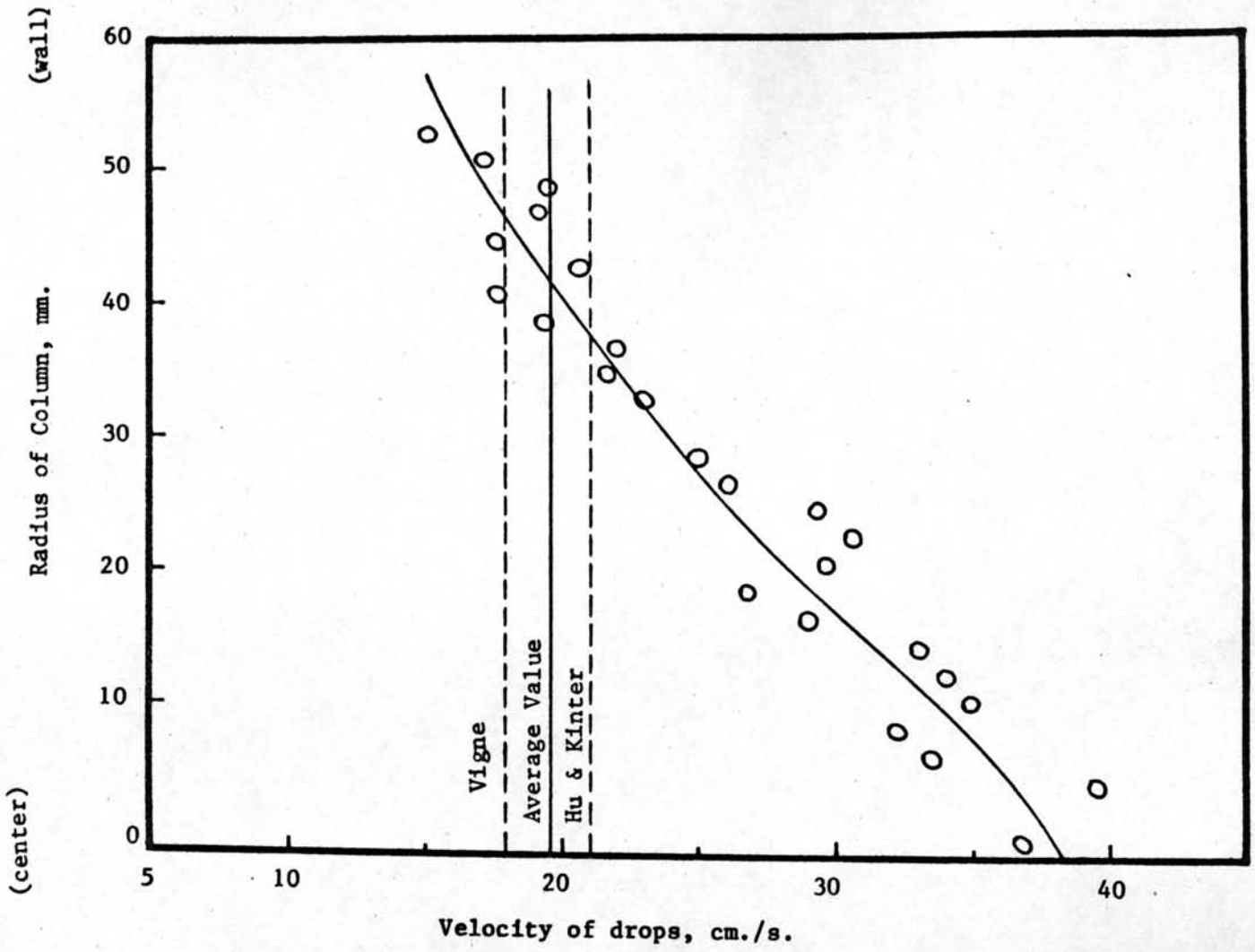

Figure 32 Velocity profile and terminal velocity of drops (distributor A flow rate 8.68 cc./s.)

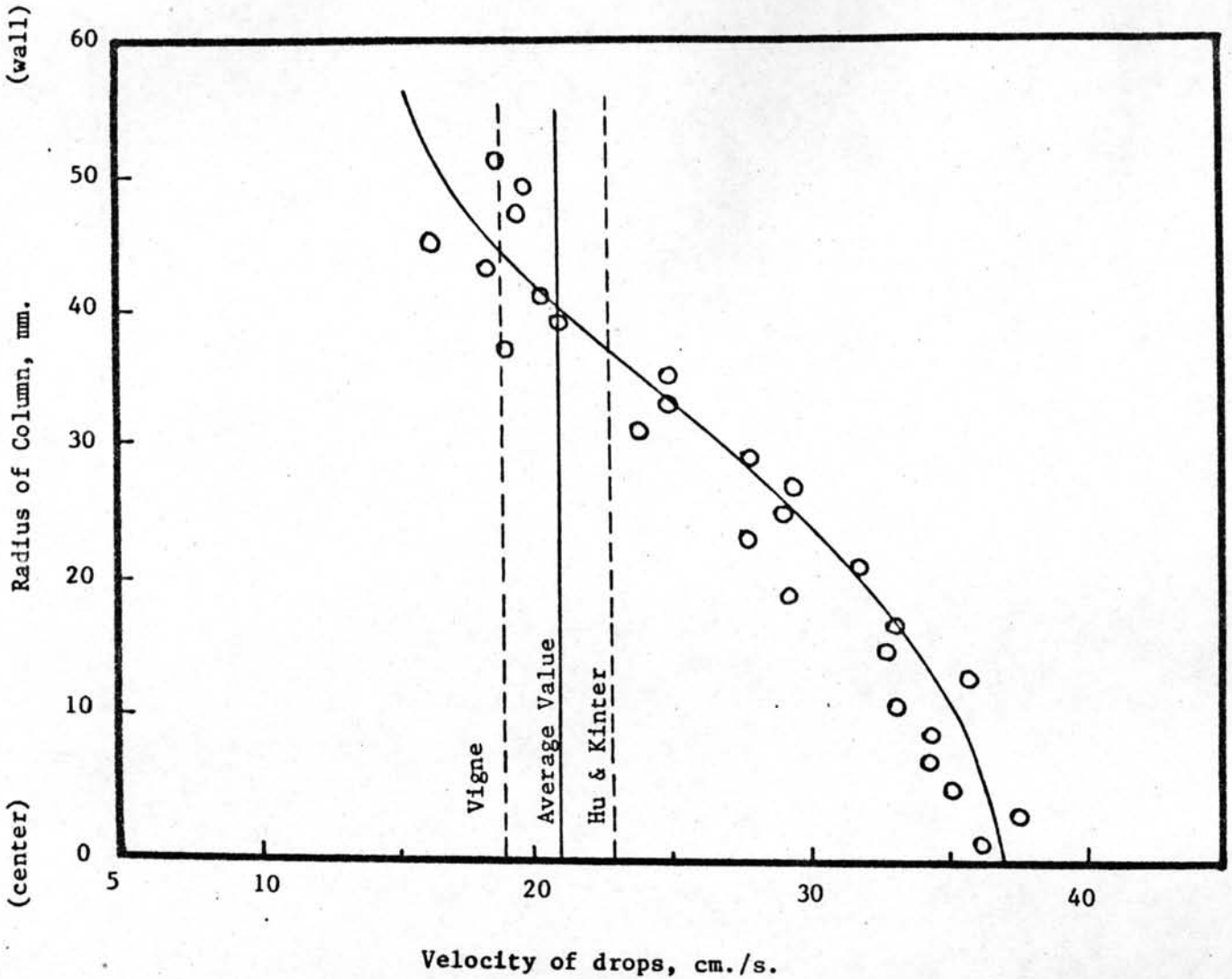

Figure 33 Velocity profile and terminal velocity of drops (distributor A flow rate 6.67 cc./s.)

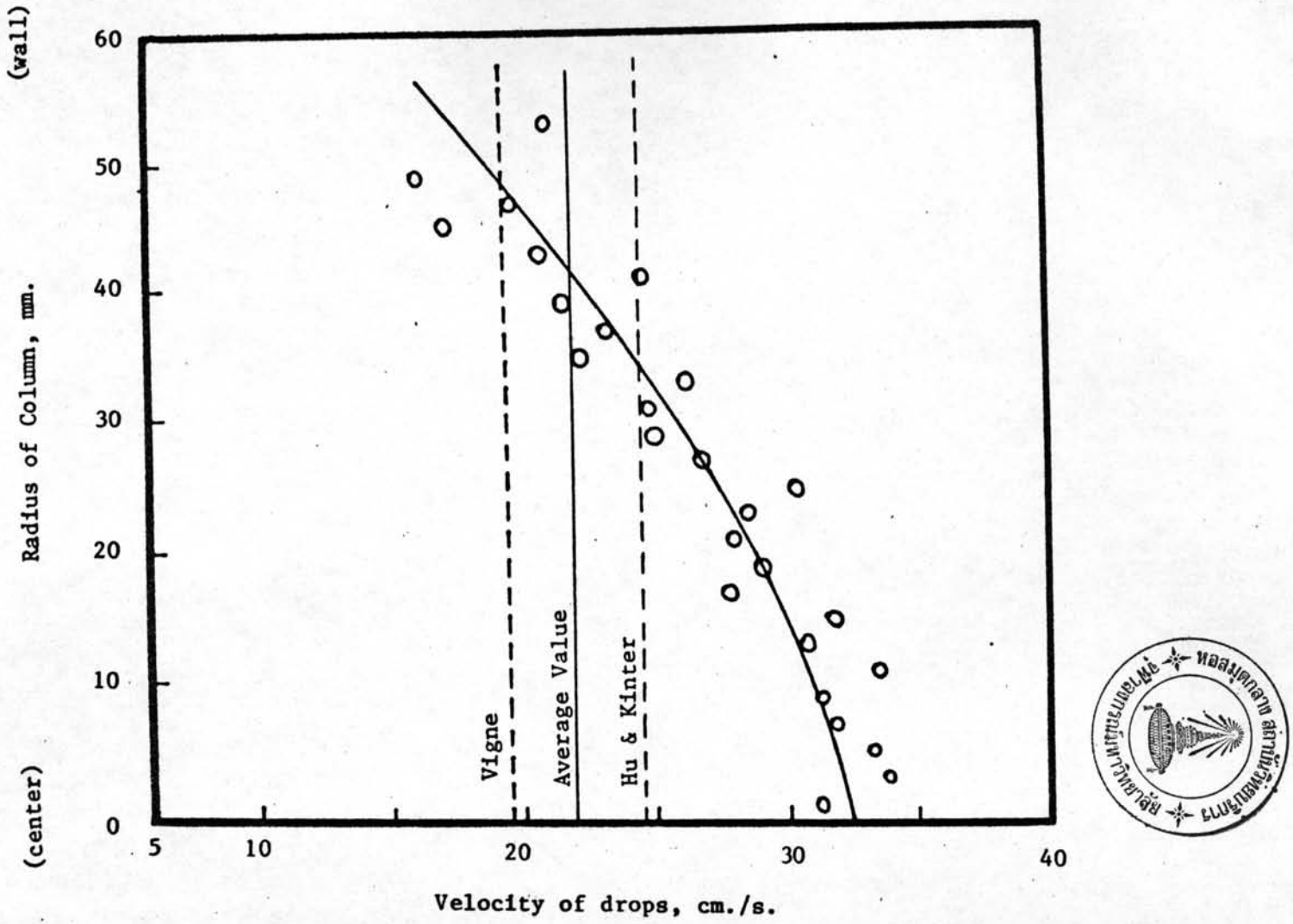

Figure 34 Velocity profile and terminal velocity of drops (distributor A flow rate 5.03 cc./s.)

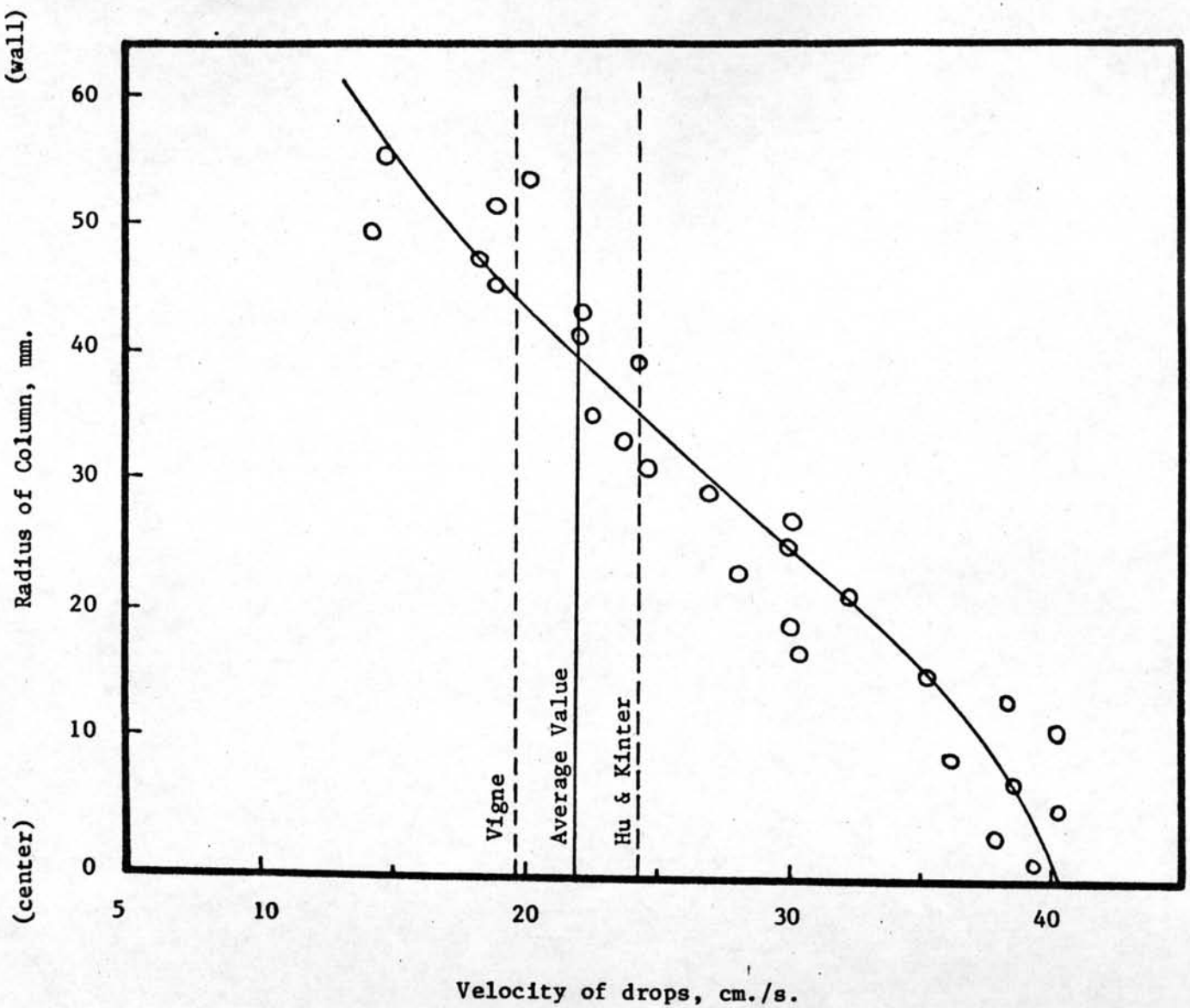

Figure 35 Velocity profile and terminal velocity of drops (distributor B flow rate 8.68 cc./s.)

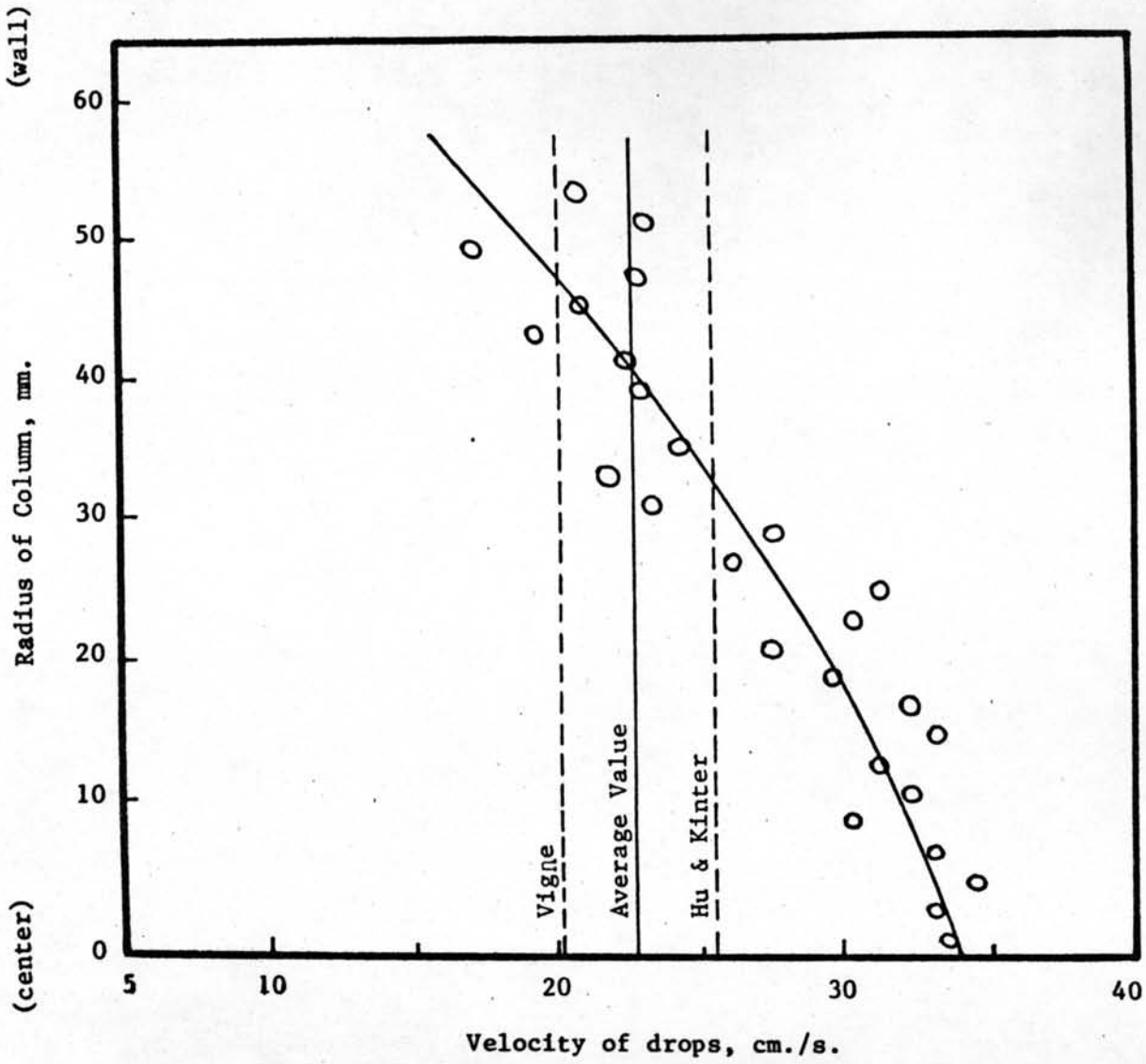

Figure 36 Velocity profile and terminal velocity of drops (distributor B flow rate 6.67 cc./s.)

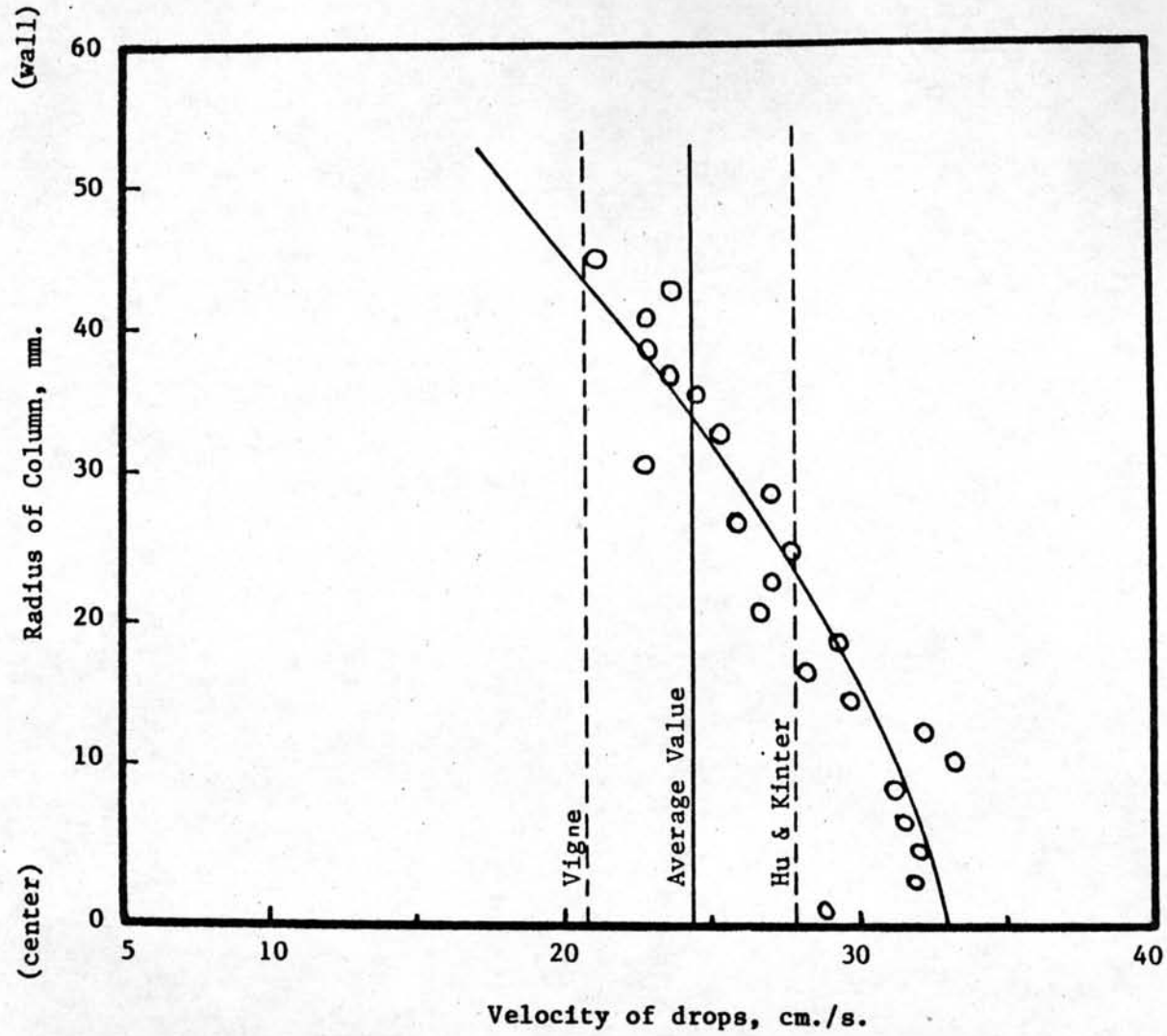

Figure 37 Velocity profile and terminal velocity of drops (distributor B flow rate 5.03 cc./s.)

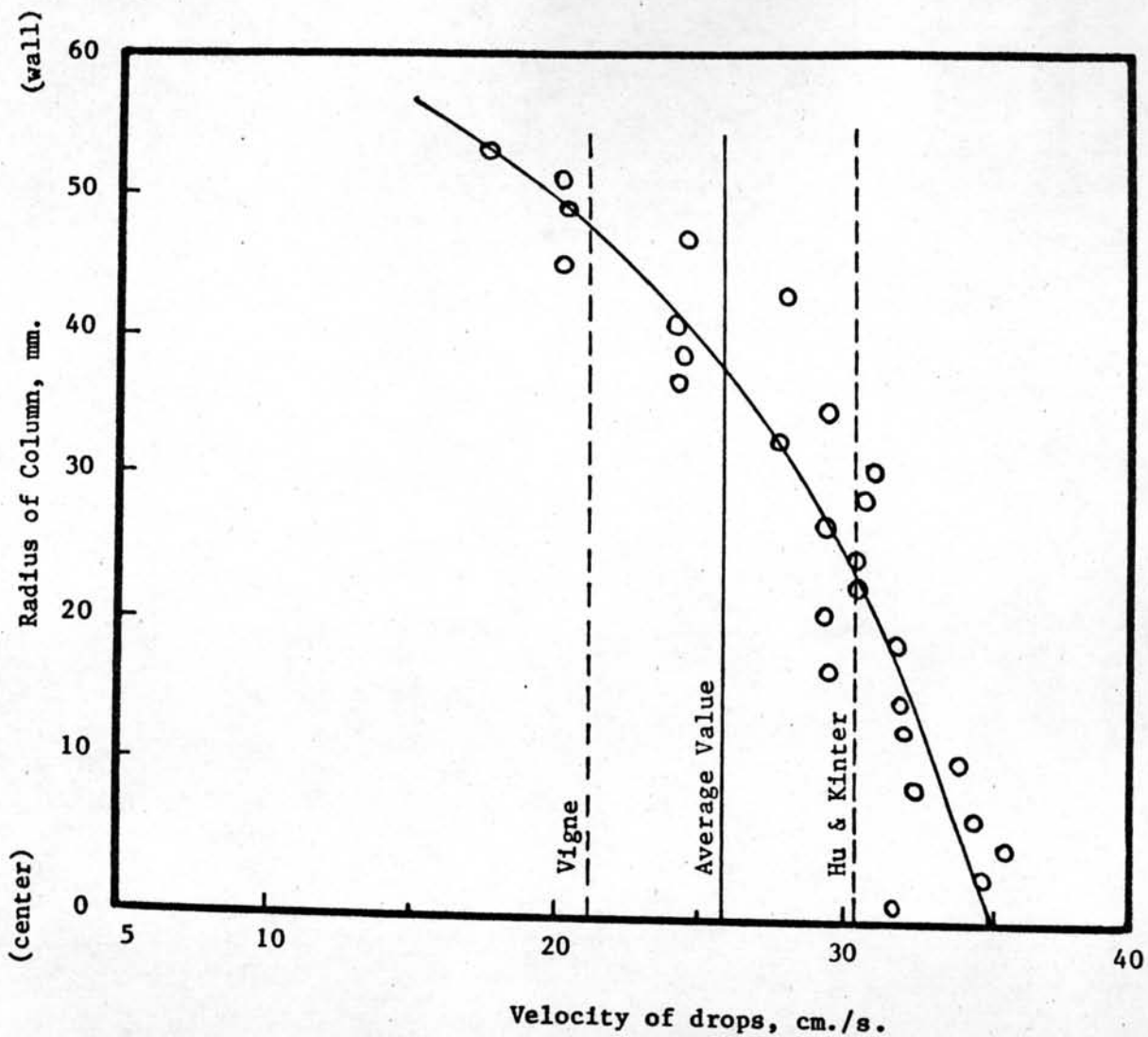

Figure 38 Velocity profile and terminal velocity of drops (distributor C flow rate 8.68 cc./s.)

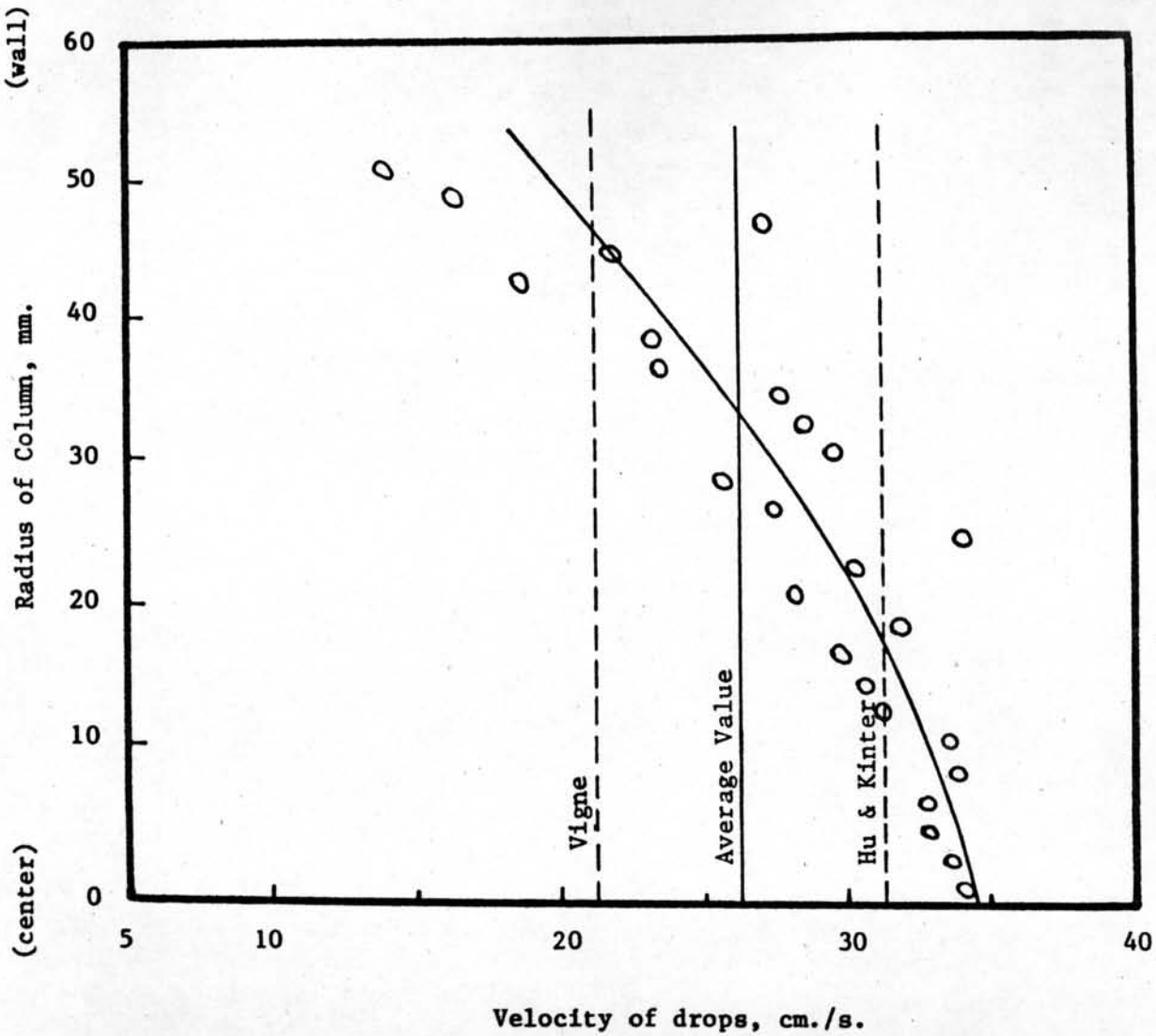

Figure 39 Velocity profile and terminal velocity of drops (distributor C flow rate 6.67 cc./s.)

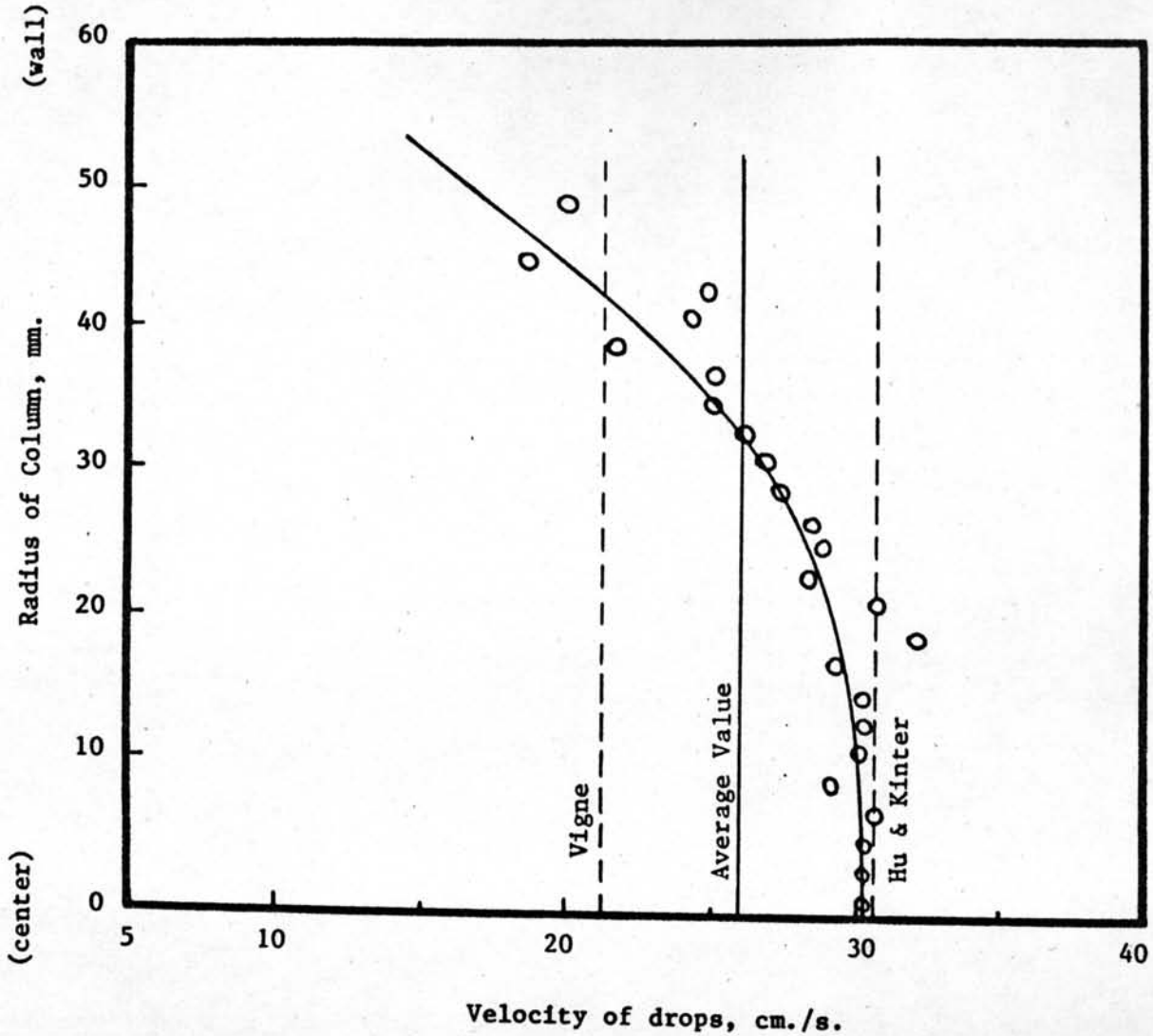

Figure 40 Velocity profile nnd terminal velocity of drops (distributor C flow rate 5.03 cc./s.)

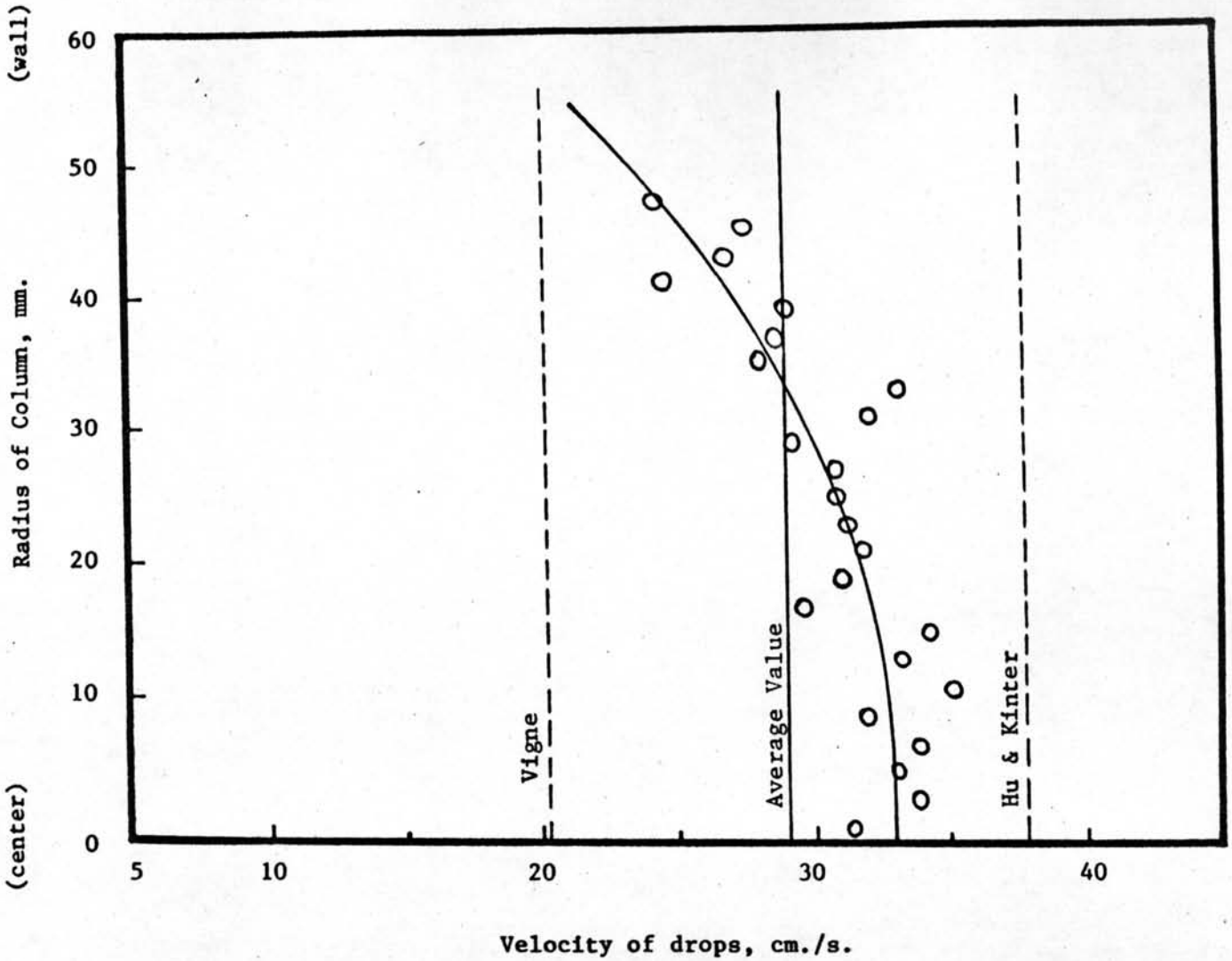

Figure 41 Velocity profile and terminal velocity of drops (distributor D flow rate 8.68 cc./s.)

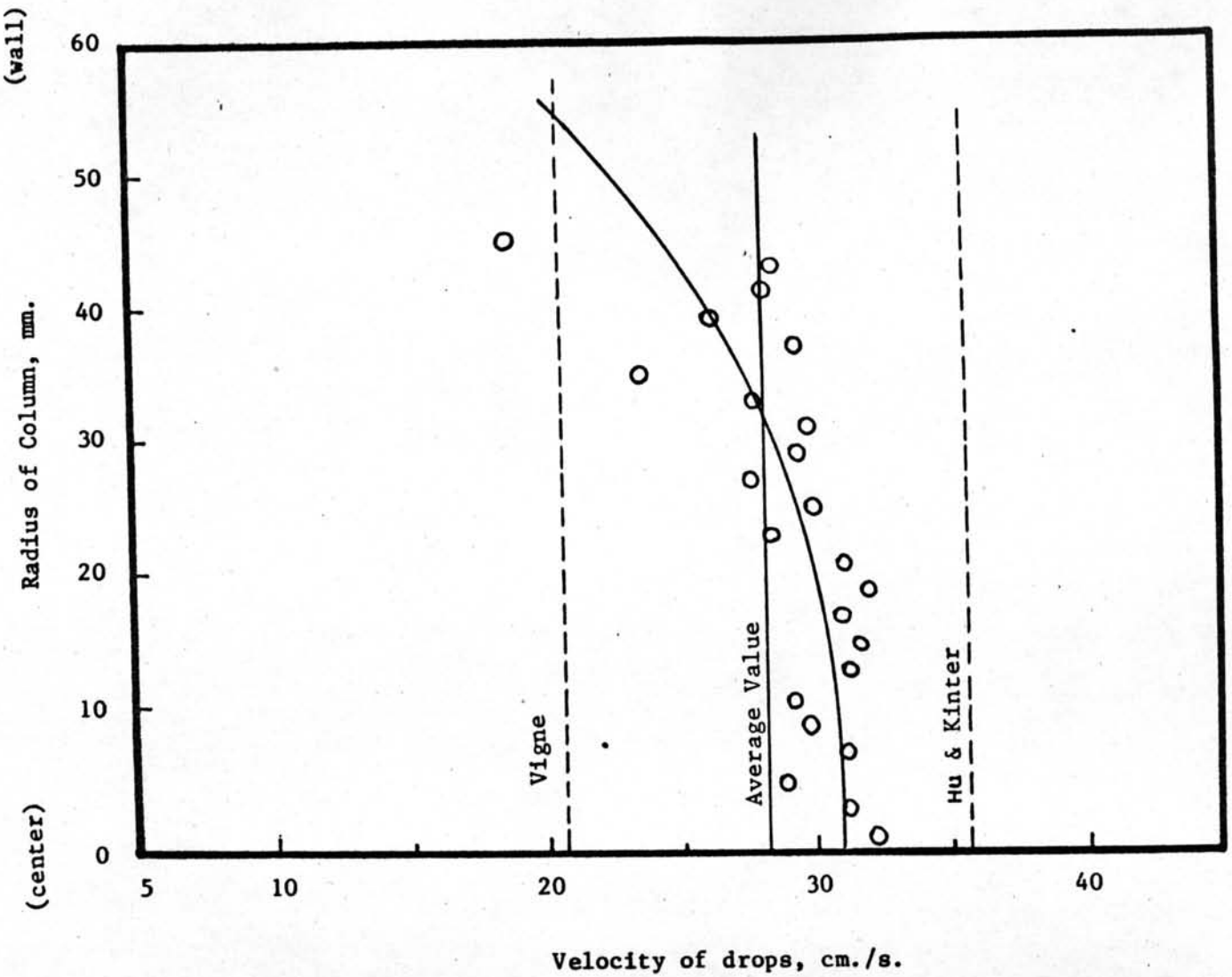

Figure 42 Velocity profile and terminal velocity of drops (distributor D flow rate 6.67 cc./s.)

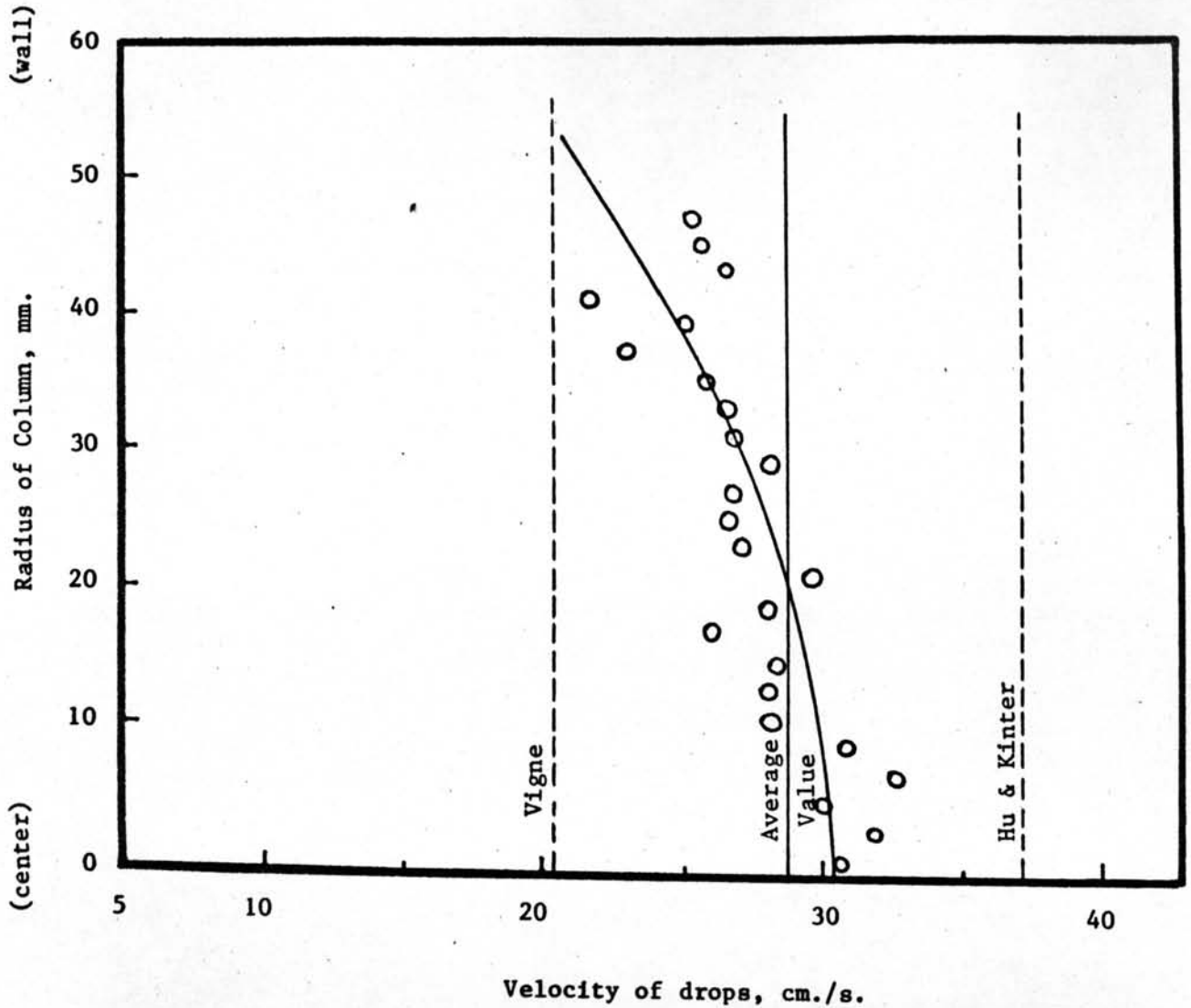

Figure 43 Velocity profile and terminal velocity of drops (distributor D flow rate 5.03 cc./s.)